The Astrophysical Journal, 648:666–682, 2006 September 1

ATMOSPHERES OF PROTOPLANETARY CORES: CRITICAL MASS FOR NUCLEATED INSTABILITY

Roman R. Rafikov[1]
Institute for Advanced Study, Einstein Drive, Princeton, NJ 08540; rrr@cita.utoronto.ca
Received 2004 May 25; accepted 2006 May 10

ABSTRACT

We systematically study quasi-static atmospheres of accreting protoplanetary cores for different opacity behaviors and realistic planetesimal accretion rates in various parts of the protoplanetary nebula. We demonstrate that there are two important classes of atmospheres: (1) those having an outer convective zone that smoothly merges with the surrounding nebular gas, and (2) those possessing an almost isothermal outer radiative region that effectively decouples the atmospheric interior from the nebula. The type of atmosphere accumulating around a given core depends on the core mass, nebular parameters, and accretion luminosity of the core. Cores in the inner parts of the protoplanetary disk (within roughly 0.3 AU from the Sun) have large luminosities resulting in atmospheres of the first type, while cores in the giant planet region (beyond several AU) have small accretion luminosities and always accumulate massive atmospheres of the second type. The critical core mass needed for the nucleated instability to commence is found to vary considerably as a function of distance from the Sun. This mass is 5–20 $M_\oplus$ at 0.1–1 AU, which is too large to permit the formation of "hot Jupiters" by nucleated instability around the cores that have grown in situ. In the region of giant planets the critical core mass depends on the gas opacity and planetesimal accretion rate but is insensitive to the nebular temperature or density provided that the opacity in the outer radiative region does not depend on the gas density (e.g., dust opacity). The critical mass in the region of giant planets can be as high as 20–60 $M_\oplus$ (for an opacity of 0.1 cm^2 g^{-1}) if planetesimal accretion is fast enough for protoplanetary cores to form prior to the nebular gas dissipation.

Subject headings: planetary systems: protoplanetary disks — planets and satellites: formation — solar system: formation

1. INTRODUCTION

One of the most popular and successful theories of giant planet formation is a core (or nucleated) instability hypothesis (Harris 1978; Mizuno et al. 1978). According to this idea, the massive hydrogen/helium atmospheres of planets like Jupiter and Saturn have been acquired as a result of unstable gas accretion onto a preexisting core made of rock and/or ice. Analytical arguments (Stevenson 1982; Wuchterl 1993) and numerical calculations (Mizuno 1980; Ikoma et al. 2000) suggest that the onset of core instability occurs when the mass of the gaseous atmosphere around the core becomes comparable to the core mass itself.

The following gedankenexperiment can help us understand the nature of this instability: imagine placing a dense protoplanetary core of mass M_p into an infinite homogeneous gaseous medium. Gravitational pull from the core gives rise to a significant pressure perturbation near the core if the escape speed from its surface is larger than the gas sound speed (see § 2.2). On a short (dynamical) timescale gas settles into a pressure equilibrium configuration near the core. Since the thermal timescale is usually longer than the dynamical timescale, initially this gaseous envelope[2] is isentropic, with an entropy equal to that of the gas in the surrounding nebula. The gas temperature at the core surface is rather high, and this drives an outward transport of energy, causing the entropy of the envelope to decrease. As a result, the gas density near the core goes up, and the envelope becomes more and more massive by slow accumulation (on a thermal timescale) of gas from the surrounding nebula.

Given enough time, the atmosphere cools down to the nebular temperature and becomes isothermal. It has an exponential density profile with most of the mass concentrated near the core (Sasaki 1989) and can be stable only if its mass $M_{\rm atm}$ is significantly smaller than M_p. This can be fulfilled only for small enough M_p, since the atmosphere accumulating around a massive core would at some point attain $M_{\rm atm} \sim M_p$ and start contributing significantly to the planetary gravity. Hydrostatic equilibrium cannot be established beyond this point, because accretion of more gas, which helps to reestablish pressure equilibrium, would also act to increase the gravitational potential. As a result, instability commences, allowing gas to accrete rapidly onto the core. The critical core mass $M_{\rm cr}$ at which instability becomes possible is thus set by the condition[3] $M_{\rm atm}(M_{\rm cr}) \sim M_{\rm cr}$. Note that if M_p is very large, or the gas around it is very dense, then even the mass of the isentropic envelope forming on the dynamical timescale after introduction of the core into the nebula might exceed M_p, making the atmosphere unstable from the very start (see § 5.3).

Real protoplanetary cores are not passive bodies of constant mass. They accrete planetesimals, and this not only increases M_p but also leads to the release of a substantial amount of energy at the surface of the core. This changes the steady state structure of the envelope, which can no longer be purely isothermal (as it would tend to become in the case of a passive core). Planetesimal accretion[4] increases the atmospheric temperature, making the gas less dense around an accreting core than around a passive core of the same mass (and lowering $M_{\rm atm}$ compared to passive

[1] Current address: CITA, McLennan Physics Labs, 60 St. George Street, University of Toronto, Toronto, ON M5S 3H8, Canada.

[2] We use the terms "envelope" and "atmosphere" interchangeably.

[3] Apart from additional logarithmic factors intrinsic to the isothermal case, see Sasaki (1989).

[4] Energy release at the core surface might also come from radioactive decay or differentiation in the core, which are not accompanied by a change in the core mass.

case). Nevertheless, similar to the case without accretion, the more massive the core is, the higher $M_{\rm atm}$ is, and the concept of a critical core mass holds again: stable equilibrium atmospheres cannot exist around cores that are so massive that $M_{\rm atm} \gtrsim M_p$.

Previous numerical and analytical studies confirmed this general picture of core instability, but there are still some open issues concerning the details of the internal structure of protoplanetary atmospheres. For example, Perri & Cameron (1974) and later Wuchterl (1993) have concluded that atmospheres are likely to be convective and that their interior structure and mass (which was found to be quite low) depend on the density and temperature of the gas in the surrounding nebula. Stevenson (1982) arrived at a very different conclusion by considering a simple analytical model of an atmosphere with a constant opacity. He found the atmosphere to be radiative and massive and its structure to be insensitive to the external conditions. His findings confirmed the previous numerical results of Harris (1978), Mizuno et al. (1978), and Mizuno (1980).

The goal of this study is to systematically explore the structure of atmospheres around accreting protoplanetary cores before they become unstable under a variety of conditions typical in the protoplanetary nebulae. Using analytically tractable but still realistic models, we single out physical parameters crucial for determining the atmospheric structure, and this provides us with a general classification scheme of possible protoplanetary atmospheres. We start by laying down the basics of the problem at hand, equations, important length and mass scales, and boundary conditions, in § 2. In §§ 3 and 4 we derive solutions for two important classes of envelope structures typical in the regions of giant and terrestrial planets. Calculation of $M_{\rm atm}$ and $M_{\rm cr}$ is presented in § 5. Our results and their implications are discussed in § 6. Finally, we devote appendices to technical issues that emerge in our calculations.

2. PROBLEM SETUP

Throughout this study the following approximation for the protoplanetary disk structure (similar to the minimum mass solar nebula [MMSN]) is used:

$$\Sigma_g(a) \approx 100\Sigma_p(a) \approx 3000 \text{ g cm}^{-2}\ a_1^{-3/2}, \quad (1)$$

$$T_0(a) \approx 300 \text{ K}\ a_1^{-1/2}, \quad (2)$$

where Σ_p and Σ_g are the particulate and gas surface densities, respectively, T_0 is the gas temperature, and $a_n \equiv a/(n \text{ AU})$ is a distance from the Sun a scaled by n AU. The nebula is vertically isothermal with a density structure $\rho(z, a) = \rho_0(a) \exp(-z^2/2h^2)$. From equation (2) we find the isothermal sound speed $c_0 \equiv (kT_0/\mu)^{1/2}$ (k is the Boltzmann constant and μ is the mean molecular weight), vertical scale height $h = c_0/\Omega$, and midplane density $\rho_0 \equiv (2\pi)^{-1/2}\Sigma_g/h$ [$\Omega \equiv (GM_\odot/a^3)^{1/2}$ is the orbital angular frequency and $M_\odot$ is the solar mass]:

$$c_0(a) \approx 10^5 \text{ cm s}^{-1}\ a_1^{-1/4}, \quad (3)$$

$$h(a)/a \approx 3.4 \times 10^{-2}\ a_1^{1/4}, \quad (4)$$

$$\rho_0(a) \approx 2.4 \times 10^{-9} \text{ g cm}^{-3}\ a_1^{-11/4}. \quad (5)$$

All numerical estimates in the text refer to this particular model of the protoplanetary disk.

2.1. *Basic Equations*

We consider a distribution of gas density ρ, pressure P, and temperature T around a protoplanetary core with mass M_p embedded in the nebular gas. We approximate the gas distribution as spherically symmetric, which requires the nebula to be at least roughly homogeneous around the core. The conditions for this to be the case are determined in § 2.3. The atmospheric structure as a function of distance r from the center of the core is governed by

$$\frac{\partial P}{\partial r} = -G\frac{M_p}{r^2}\rho. \quad (6)$$

Here we have assumed $M_p \gtrsim M_{\rm atm}$. This restricts our quantitative results to cores that are subcritical, although all qualitative conclusions are valid by extrapolation even for $M_p \sim M_{\rm cr}$, a fact that we use to estimate M_p in § 5.3. Equation (6) assumes that the atmosphere is not rapidly rotating.

The atmosphere is heated from below by a source at the core surface (radius R_p) with a luminosity

$$L = G\frac{M_p\dot{M}}{R_p}, \quad (7)$$

which is derived from planetesimal accretion at the rate $\dot{M}$ (we neglect additional energy release due to the radioactive heating and differentiation inside the core). In Appendix A we briefly summarize three different regimes of planetesimal accretion important for the core growth and calculate $\dot{M}$ and the accretion timescale for each of them. Equation (7) assumes that (1) the planetesimal velocity far from the core is small compared to the core's escape speed, and (2) planetesimals penetrate to the core surface without much resistance from the envelope and release there all their kinetic energy. The first assumption is almost certainly fulfilled during the buildup of the core by planetesimal accretion; the second should be valid for large planetesimals, but small ones may be slowed down by the gas drag in the envelope as they make their way to the core surface. In the latter case the accretion energy release does not occur exactly at the core surface but is distributed throughout the envelope, meaning that luminosity depends on r. However, even in the most unfavorable case of small planetesimals that are quasi-statically lowered from the top of the atmosphere to its bottom, the luminosity is $(1 - R_p/r)L$, i.e., the luminosity varies only very near the core's surface (Pollack et al. 1996). At $r \gtrsim R_p$, in the bulk of the atmosphere, we can safely assume L to be a constant given by equation (7).

The accretion luminosity is transported by radiative diffusion or convection. According to the Schwarzschild criterion, the atmosphere is convectively stable when

$$\nabla < \nabla_{\rm ad} \equiv \frac{\gamma - 1}{\gamma}, \quad \nabla \equiv \frac{\partial \ln T}{\partial \ln P}, \quad (8)$$

where ∇ is the temperature gradient and $\nabla_{\rm ad}$ is its value under isentropic conditions, and γ is the adiabatic index of the gas (for monatomic gas $\nabla_{\rm ad} = 2/5$, and for diatomic, e.g., H_2, $\nabla_{\rm ad} = 2/7$). Use of the Schwarzschild criterion implies that the envelope is chemically homogeneous and nonrotating; a more general Ledoux criterion should be used in the presence of molecular weight gradients (Kippenhahn & Weigert 1990), and the Høiland criterion has to be employed if the envelope rotates rapidly (Tassoul 1978).

When atmosphere is convectively stable according to equation (8), energy released at the core surface is carried away radiatively. In this case one supplements equation (6) with the

equation of radiation transfer. In the diffusion approximation, valid in the optically thick[5] case, it reads

$$\frac{16\sigma T^3}{3\kappa\rho}\frac{\partial T}{\partial r} = -\frac{L}{4\pi r^2}, \tag{9}$$

where σ is the Stefan-Boltzmann constant and κ is the opacity. We consider a rather general opacity law by assuming throughout this work that

$$\kappa = \kappa_0 (P/P_0)^{\alpha} (T/T_0)^{\beta}, \tag{10}$$

where κ_0, P_0, and T_0 are the opacity, pressure, and temperature in the nebular gas far from the core. In the upper atmosphere the opacity is dominated by dust, and the exact value of κ_0 is highly uncertain because the amount of dust and its size distribution are poorly constrained in protoplanetary disks. Thus, we treat κ_0 as a parameter and for simplicity assume it to be independent of a.

All previous studies (Mizuno 1980; Stevenson 1982) assumed κ to be constant, independent of P or T. However, at long wavelengths dust grains are known to produce a temperature-dependent opacity $\kappa \propto T^{\beta}$ (i.e., $\alpha = 0$) with $\beta \approx 1$–2 (Draine 2003, 2006). Our prescription (10) accounts for this possibility and is more general compared to previous treatments. The detailed behavior of κ in the deep atmosphere (likely dominated by the molecular opacity of H_2 and H_2O, for which one has to use opacity tables) may not be so important for determining the atmospheric structure or mass, since the atmosphere can be convective there (see § 6.1).

Whenever the stability criterion (8) is violated, energy in the envelope is transported by convection. We assume convection to be effective, so that $\nabla \approx \nabla_{\rm ad}$. This is equivalent to supplementing equation (6) with an isentropic equation of state

$$P = K\rho^{\gamma}, \tag{11}$$

where K is the adiabatic constant, a measure of the gas entropy. This approximation should be very good for dense atmospheres (e.g., interiors of present-day giant planets). In Appendix D we determine under what circumstances this assumption is valid in the atmospheres of protoplanetary cores.

Use of the steady state equations (6) and (9) tacitly assumes that the envelope quickly adjusts to the changes in the core mass M_p and luminosity L caused by planetesimal accretion. In other words, these equations hold only provided that the dynamical and thermal timescales of the atmosphere are shorter than the core accretion timescale $M_p/\dot{M}$. In Appendix C we demonstrate this assumption to be reasonable. We also show in § 6.3 that in the framework of the quasi-stationary approximation the rate of energy release by gas accretion is small compared to the planetesimal accretion luminosity in equation (7).

2.2. *Important Length Scales*

There are several characteristic length scales important for the problem at hand. Some of them are independent of the core's presence:

1. The vertical scale height h given by equation (4) determines the geometric thickness of the disk.

2. The mean free path of photons in the nebular gas,

$$\lambda \equiv (\kappa_0\rho_0)^{-1} \approx 1.7\times10^9 \text{ cm } a_1^{11/4}\kappa_{0.1}^{-1}, \tag{12}$$

determines whether the disk is optically thick ($\lambda \lesssim h$) or thin ($\lambda \gtrsim h$). Here $\kappa_{0.1} \equiv \kappa_0/0.1$ cm^2 g^{-1}.

Other length scales are relevant only in the presence of planet:

1. The Hill radius

$$R_{\rm H} \equiv a\left(\frac{M_p}{M_\odot}\right)^{1/3} \approx 2\times10^{11} \text{ cm } a_1 \left(\frac{M_p}{M_\oplus}\right)^{1/3} \tag{13}$$

is a measure of the relative importance of the core gravity compared to the tidal field of the central star. Within the Hill sphere ($r \lesssim R_{\rm H}$) the dynamics is determined primarily by the gravity of the core, while outside of it stellar gravity dominates.

2. The Bondi radius

$$R_{\rm B} \equiv G\frac{M_p}{c_0^2} \approx 4\times10^{10} \text{ cm } a_1^{1/2}\ \frac{M_p}{M_\oplus} \tag{14}$$

is defined as the distance from the protoplanet at which the thermal energy of the nebular gas is of the order of its gravitational energy in the potential well of the core. Outside the Bondi sphere (for $r \gtrsim R_{\rm B}$) the gravity of the core is too weak to affect the gas and $P \approx P_0$. Inside the Bondi sphere the pressure is significantly perturbed by the gravity of the core.

3. The physical radius of the protoplanetary core

$$R_p \equiv \left(\frac{3}{4\pi}\frac{M_p}{\rho_p}\right)^{1/3} \approx 10^9 \text{ cm}\left(\frac{M_p}{M_\oplus}\right)^{1/3}\rho_1^{-1/3} \tag{15}$$

scales with M_p in the same way as $R_{\rm H}$, meaning that their ratio p depends only on the physical density of the core ρ_p and the distance from the star:

$$p \equiv \frac{R_p}{R_{\rm H}} = \left(\frac{3}{4\pi}\frac{M_\odot}{\rho_p a^3}\right)^{1/3} \approx 5.2\times10^{-3}\ a_1^{-1}\ \rho_1^{-1/3}, \tag{16}$$

where $\rho_1 \equiv \rho_p/(1 \text{ g cm}^{-3})$. Clearly, $R_p \ll R_{\rm H}$.

4. The luminosity radius of the core

$$R_L \equiv \left(\frac{L}{16\pi\sigma T_0^4}\right)^{1/2} \tag{17}$$

is 1/2 of the radius of the sphere that can radiate the accretion luminosity L at an effective temperature T_0.

In Figure 1 we plot different length scales as functions of a for two values of M_p and for different accretion regimes (see Appendix A).

One can define the "sphere of influence" of protoplanetary core as the region of space in which planetary gravity dominates over both the tidal field of the Sun and the unperturbed nebular pressure P_0. Clearly, the size of this sphere is $\min(R_{\rm B}, R_{\rm H})$, and inside it the gas dynamics is determined only by the gravity of the core and pressure gradients in the surrounding gas.

2.3. *Important Mass Scales*

The existence and geometry of the protoplanetary atmosphere introduce two important mass scales.

[5] In the outer solar system gas around a protoplanet can be so rarefied that outer parts of the atmosphere become optically thin. This possibility is considered in more detail in § 3.2.

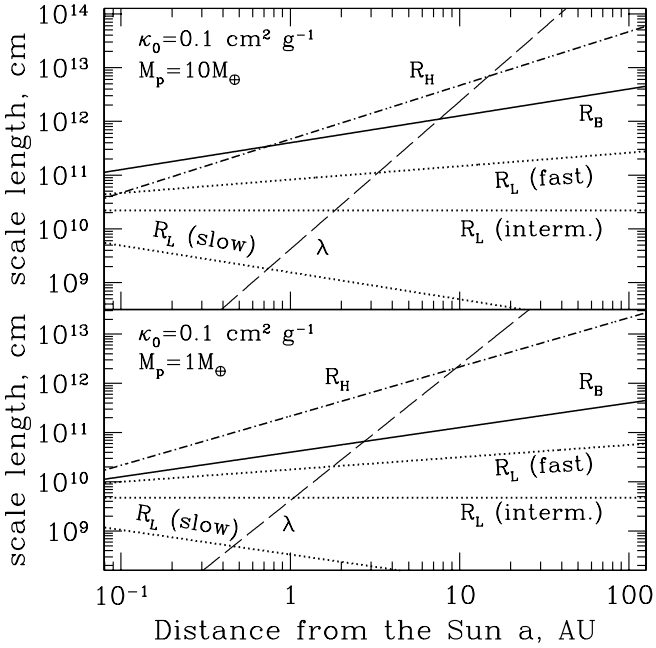

FIG. 1.—Different length scales important for atmospheric structure as functions of semimajor axis a for $\kappa_0 = 0.1$ cm^2 g^{-1} and two values of the core mass: $M_p = 10\,M_\oplus$ (*top*) and $M_p = 1\,M_\oplus$ (*bottom*). Solid, dashed, and dot-dashed lines represent R_B, λ, and R_H, respectively. Dotted lines correspond to the luminosity radius R_L evaluated for three different planetesimal accretion regimes, fast, intermediate, and slow (see Appendix A), labeled on the plot.

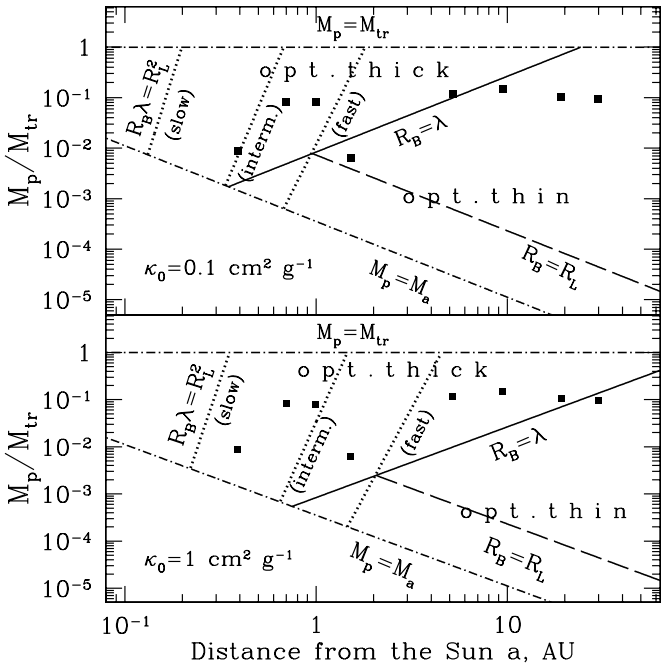

FIG. 2.—Relationships between different length scales as a function of semimajor axis a in the nebula for two values of the gas opacity (assumed constant throughout the nebula): $\kappa_0 = 0.1$ cm^2 g^{-1} (*top*) and $\kappa_0 = 1$ cm^2 g^{-1} (*bottom*). Only the case $M_a < M_p < M_{tr}$ is considered (*dot-dashed boundaries*). Dotted lines correspond to the condition $R_B\lambda = R_L^2$ for three different planetesimal accretion regimes labeled on the curves. The solid line represents $R_B = \lambda$ separating optically thick and optically thin atmospheres (see §§ 3.1 and 3.2), while the dashed line is for $R_B = R_L$. Squares mark the positions of the eight major planets of the solar system; for Jupiter and Saturn we assume cores of 5 and 10 $M_\oplus$.

1. The core possesses an atmosphere only if $R_B \gtrsim R_p$ or, equivalently, when $M_p \gtrsim M_a$, where

$$M_a \equiv \frac{c_0^3}{G}\left(\frac{3}{4\pi G\rho_p}\right)^{1/2} \approx 4.5\times10^{-3}\ M_\oplus\ a_1^{-3/4}\ \rho_1^{-1/2}. \quad (18)$$

If $M_p \lesssim M_a$, then even at the surface of the core the thermal energy of the nebular gas is greater than its potential energy in the core's gravitational field, so that gas is almost unperturbed at $r = R_p$ (i.e., $R_B \lesssim R_p$). In this case the very concept of an atmosphere loses its meaning. We do not consider such low-mass cores.

2. The nebula can be considered homogeneous on the scale of R_B only if $R_B \ll h$ (so that the Bondi sphere is confined within the core of the Gaussian profile of the vertical gas density distribution). This requires that $M_p \lesssim M_{tr}$, where the *transitional* mass M_{tr} is defined as

$$M_{tr} \equiv \frac{c_0^3}{G\Omega} \approx 12\ M_\oplus\ a_1^{3/4}. \quad (19)$$

One can easily see that whenever this condition is fulfilled R_B is also smaller than R_H, while $R_H \lesssim h$. In the opposite case, when $M_p \gtrsim M_{tr}$, the Bondi sphere extends beyond the Hill sphere ($R_B \gtrsim R_H$), while the gas within the Hill sphere is very inhomogeneously[6] distributed, since $R_H \gtrsim h$. At 10 AU $M_{tr} \approx 70\,M_\oplus$, while at 30 AU $M_{tr} \approx 150\,M_\oplus$.

In this study we only consider cores with masses satisfying

$$M_a \lesssim M_p \lesssim M_{tr}, \quad (20)$$

for which the following hierarchy holds:

$$R_p \lesssim R_B \lesssim R_H \lesssim h, \quad (21)$$

i.e., the cores that are massive enough to have an atmosphere but still small enough for their atmospheres to have at least rough spherical symmetry (within the sphere of influence, which in this case coincides with the Bondi sphere). This restriction allows us to avoid discussing the complicated morphology and dynamics of an atmosphere corresponding to the case $M_p \gtrsim M_{tr}$.

Since according to equations (18) and (19) $M_a = p^{3/2}M_{tr}$, there is a broad mass range in which equation (20) can be valid, spanning 4–5 orders of magnitude in mass depending on a (e.g., from $\sim$0.1 lunar mass to $\sim M_J$ at 10 AU). In Figure 2 we show how different length scales are related to each other as functions of a and M_p/M_{tr}, constrained by equation (20).

2.4. *Boundary Conditions*

Boundary conditions to the equations of § 2.1 specify that the gas pressure, temperature, and density should reduce to their nebular values P_0, T_0, and ρ_0 at some distance R_{out} from the core:

$$T(R_{out}) = T_0, \quad P(R_{out}) = P_0, \quad \rho(R_{out}) = \rho_0. \quad (22)$$

Apparently, pressure may converge to P_0 only beyond R_B, so that $R_{out} \gtrsim R_B$. If one neglects the differential motion of gas outside the protoplanetary sphere of influence caused by the gravity of the central star and assumes the gas to be static everywhere, then R_{out} can be set equal to infinity. The presence of the shearing motion in the disk changes the gas dynamics in the vicinity of the core, as even inside the Hill sphere gas can move in a rather complicated fashion, as demonstrated by hydrodynamic

[6] When condition (19) is violated, a gap can form around the planetary orbit (Lin & Papaloizou 1993; Rafikov 2002), additionally complicating the geometry of the protoplanetary atmosphere.

simulations of planet-disk interaction (e.g., D'Angelo et al. 2002, 2003). In addition, the flow of unbound nebular gas within the Hill sphere can effectively "cool" the outer part of the protoplanetary atmosphere by advecting the gas heated by the core luminosity away from it and bringing in fresh gas having an entropy equal to the nebular entropy. If this process were setting the temperature boundary condition, then $R_{\rm out} \gtrsim R_{\rm B}$, since within the Bondi sphere gas is confined by the core's gravity and is not being refreshed. In reality, our self-consistent solutions for the structure of the protoplanetary atmospheres (§§ 3 and 4) almost always have $T \approx T_0$ already at $r \sim R_{\rm B}$.

A proper estimate of $R_{\rm out}$ must account for the complicated geometry of the flow near the core, the vertical structure of the nebula, the possibility of forming a rotationally supported disk around the core, the inhomogeneous heating within $R_{\rm out}$, and so on. Fortunately, provided that $M_p \lesssim M_{\rm tr}$ (i.e., $R_{\rm B} \lesssim R_{\rm H}$), one should expect the sphere of influence of the protoplanet to be more or less isolated from these complicated effects. It turns out (see § 6.3) that as long as $R_{\rm out} \gtrsim R_{\rm B}$, the exact value of $R_{\rm out}$ is not important for the structure of the atmosphere. For this reason in our calculations we simply set $R_{\rm out} = 20 R_{\rm B}$.

3. ATMOSPHERES WITH OUTER RADIATIVE ZONE

Figure 2 demonstrates that for protoplanetary cores with $M_p \approx$ 1–10 $M_\oplus$ at $a \gtrsim$ 2–5 AU accreting planetesimals in the fast regime, either

$$\lambda \ll R_{\rm B}, \quad R_L^2 \ll \lambda R_{\rm B} \tag{23}$$

or

$$R_L \ll R_{\rm B} \ll \lambda \tag{24}$$

is typically fulfilled depending on a and κ_0. For smaller cores or less vigorous planetesimal accretion these conditions can be satisfied even closer to the Sun. Hereafter we call objects for which either equation (23) or (24) holds "low-luminosity" cores.

Under these assumptions the energy released near the surface of the core must be carried away by radiation at least in the upper atmosphere. Indeed, using equations (6), (8), and (9), one finds

$$\begin{aligned}\nabla(T) &= \frac{3}{64\pi}\frac{L\kappa_0\rho_0 c_0^2}{GM_p\sigma T_0^4}\left(\frac{T}{T_0}\right)^{\beta-4}\left(\frac{P}{P_0}\right)^{1+\alpha} \\ &= \nabla_\infty\left(\frac{T}{T_0}\right)^{\beta-4}\left(\frac{P}{P_0}\right)^{1+\alpha},\end{aligned} \tag{25}$$

where

$$\nabla_\infty = \frac{3}{4}\frac{R_L^2}{R_{\rm B}\lambda} \tag{26}$$

is the temperature gradient far from the core, outside its Bondi sphere (where $P = P_0$ and $T = T_0$). Whenever equation (23) or (24) is fulfilled, $\nabla_\infty \ll 1$, so that the atmosphere is convectively stable at $r \gtrsim R_{\rm B}$ according to equation (8).

3.1. *Low-Luminosity, Optically Thick Case ($\lambda \lesssim R_{\rm B}$ and $R_L^2 \ll \lambda R_{\rm B}$)*

Whenever $\lambda \lesssim R_{\rm B}$, the atmosphere is everywhere optically thick. In this case its structure is completely determined by equations (6) and (9). Integrating them together with equation (10) and using the boundary condition $P = P_0$ when $T = T_0$, one finds

$$\left(\frac{P}{P_0}\right)^{1+\alpha} - 1 = \frac{\nabla_0}{\nabla_\infty}\left[\left(\frac{T}{T_0}\right)^{4-\beta} - 1\right], \tag{27}$$

$$\nabla_0 \equiv \frac{1+\alpha}{4-\beta}. \tag{28}$$

The meaning of the constant ∇_0 will become clear later on (see § 3.3). Whenever T increases with depth, $\nabla_0 > 0$, and we assume this to be the case in this study. The coefficient on the right-hand side of equation (27) is very large because of equation (23), so that a large change of P results in only a small perturbation of T.

To make further progress, we need to substitute equation (27) into either equation (6) or equation (9) and find $P(r)$ and $T(r)$, which can be done numerically for arbitrary α and β. Here we look for the asymptotic behavior of the atmospheric properties in two regions: in the "outer atmosphere," where $T - T_0 \lesssim T_0$, and in the "deep atmosphere," where one expects $T \gg T_0$.

In the first case $T \approx T_0$, and one obtains using equations (6) and (27)

$$\frac{P}{P_0} \approx \frac{\rho}{\rho_0} \approx \exp\left(\frac{R_{\rm B}}{r} - \frac{R_{\rm B}}{R_{\rm out}}\right), \tag{29}$$

$$\frac{T - T_0}{T_0} \approx \frac{\nabla_\infty}{(1+\alpha)}\left\{\exp\left[(1+\alpha)\left(\frac{R_{\rm B}}{r} - \frac{R_{\rm B}}{R_{\rm out}}\right)\right] - 1\right\}, \tag{30}$$

where we have used the boundary conditions in equation (22). One can see that while ρ and P grow exponentially inside the Bondi sphere, the temperature perturbation is small at $r \sim R_{\rm B}$ because of our assumption $R_{\rm B}\lambda/R_L^2 \sim \nabla_\infty^{-1} \gg 1$. Only when the distance to the core center becomes as small as

$$R_a \equiv R_{\rm B}\frac{1+\alpha}{\ln\left(R_{\rm B}\lambda/R_L^2\right)} \approx R_{\rm B}\frac{1+\alpha}{\ln\left(\nabla_\infty^{-1}\right)} \tag{31}$$

does one find that $T - T_0 \sim T_0$. Apparently, $R_a \ll R_{\rm B}$, although one should keep in mind that the dependence of R_a on $R_{\rm B}\lambda/R_L^2$ is only logarithmic. The pressure P_a and density ρ_a at this depth are

$$\frac{P_a}{P_0} \approx \frac{\rho_a}{\rho_0} \approx \nabla_\infty^{-1/(1+\alpha)} \gg 1. \tag{32}$$

The existence of the outer radiative layer, in which $T \approx T_0$ while the density dramatically increases, was first found numerically by Harris (1978) under the conditions typical in the region of giant planets. Note that the presence of the outer isothermal layer does not necessarily require the gas to be optically thin (cf. Mizuno et al. 1978).

In the deep atmosphere, interior to R_a, we use the limit $T \gg T_0$ to integrate equation (9) with equation (27). Using $T \approx \xi T_0$ ($\xi \sim 1$) at $r = R_a$ as an approximate boundary condition at the transition point between the two asymptotic regimes, one finds a radiative zero solution

$$\frac{T}{T_0} \approx \xi + \nabla_0\left(\frac{R_{\rm B}}{r} - \frac{R_{\rm B}}{R_a}\right), \tag{33}$$

$$\frac{P}{P_0} \approx \left(\frac{\nabla_0}{\nabla_\infty}\right)^{1/(1+\alpha)}\left[\xi + \nabla_0\left(\frac{R_{\rm B}}{r} - \frac{R_{\rm B}}{R_a}\right)\right]^{1/\nabla_0}. \tag{34}$$

In the case of constant opacity ($\alpha = \beta = 0$, $\nabla_0 = 1/4$) at $r \ll R_a$, this solution reduces to that found by Stevenson (1982).

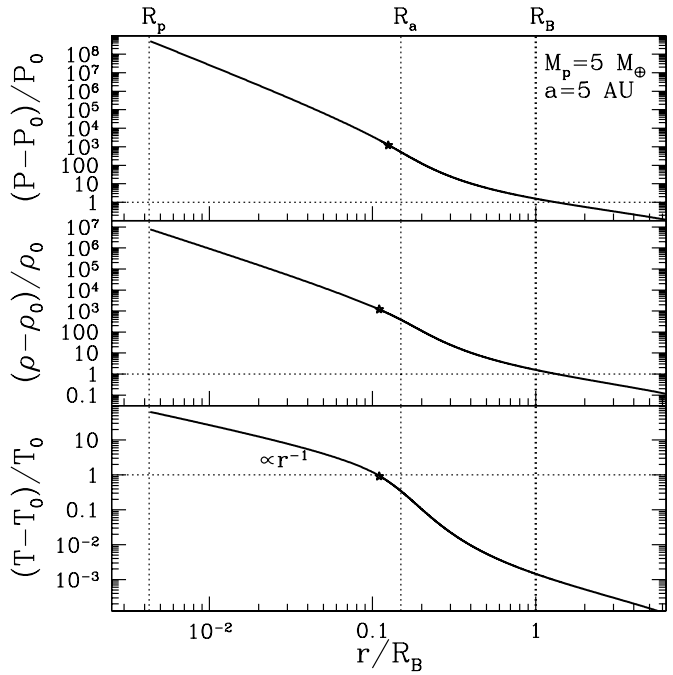

FIG. 3.—Atmospheric structure around the core with $M_p = 5\ M_\oplus$ at 5 AU. Relative deviations of P, ρ, and T from their nebular values are shown ($P_0 = 1.3 \times 10^{-7}$ bar, $\rho_0 = 3 \times 10^{-11}$ g cm^{-3}, and $T_0 = 130$ K in the surrounding nebula). The calculation is done for $\alpha = 0$, $\beta = 1$, $\gamma = 7/5$, and $\kappa = 0.1$ cm^2 g^{-1}; planetesimal accretion in the intermediate regime is assumed. In this particular case $\lambda < R_B$ and $R_B\lambda/R_L^2 \approx 800$, i.e., the envelope is optically thick everywhere and has an outer radiative zone (see § 3.1). Stars mark the position of the outer edge of the inner convective region.

Figure 3 shows the internal structure of an atmosphere around a 5 $M_\oplus$ core at 5 AU (for which eq. [23] is valid) calculated using equations (6) and (27). An opacity with $\alpha = 0$, $\beta = 1$, and $\kappa_0 = 0.1$ cm^2 g^{-1}, as well as $\gamma = 7/5$, are assumed in this calculation, and we use planetesimal accretion in the intermediate regime. The adopted scaling of κ with P and T makes the inner part of the envelope convective below R_a (see § 3.3) so that equations (33) and (34) do not apply, but this hardly changes the overall picture of the atmospheric structure described above.

3.2. *Low-Luminosity, Optically Thin Case ($R_L \ll R_B \lesssim \lambda$)*

Whenever $\lambda \gtrsim R_B$, there is an optically thin region around the protoplanet where λ exceeds the scale over which physical variables such as P and T vary. Deep in the atmosphere (below the photosphere) the gas becomes optically thick because of the increasing density. The nebula is also optically thick far from the core,[7] at $r \gtrsim \lambda$. Thus, the optically thin zone around the core surrounded by the homogeneous nebula is sandwiched between the inner and outer optically thick regions.

The temperature in the optically thick parts is determined by equation (9). In the optically thin region $T^4 \approx T_0^4 + L/(16\pi\sigma r^2)$, where an additional factor of 4 in the denominator of the second term comes from the anisotropy of the core radiation. Similar behavior of T in the optically thin region was found by Hayashi et al. (1979). Strictly speaking, this expression is accurate only far from the photosphere, and we should expect it to reproduce the photospheric temperature only approximately (which will not affect our results in any significant way). Interpolating between the outer optically thick and intermediate optically thin regions, we find T above the photosphere to be given by

$$T^4(r) \approx T_0^4 + \frac{L}{16\pi\sigma r^2} + \frac{3L}{16\pi\sigma}\int_r^\infty \frac{\kappa\rho(r')\,dr'}{r'^2}. \quad (35)$$

The third term on the right-hand side becomes important outside of $r \approx \lambda$, where photons couple to the nebular gas and diffuse.

Under assumption (24), one finds from equation (35) that

$$T(r) \approx T_0\left(1 + \frac{R_L^2}{r^2} + 3\frac{R_L^2}{\lambda r}\right)^{1/4} \quad (36)$$

for $r \gtrsim R_B$. Clearly, the temperature perturbation at the Bondi sphere $T(R_B) - T_0 \sim T_0(R_L/R_B)^2$ is negligible, similar to the optically thick case considered in § 3.1. This result is independent of whether λ is larger or smaller than h or R_H; what is crucial is that $R_L \ll R_B \ll \lambda$ (the third term in eq. [36] is negligible compared to the second at $r \sim R_B$).

Inside the Bondi sphere the gas is initially optically thin with T still given by equation (36), while P and ρ grow exponentially in accordance with equation (29) in this essentially isothermal region. As a result, the local photon mean free path rapidly decreases, and the gas finally becomes optically thick to the escaping radiation. The radius of the photosphere R_{ph} is determined by the condition that the photon mean free path $(\kappa\rho)^{-1}$ becomes comparable to the pressure scale height $\partial r/\partial \ln P = r^2/R_B$ (see eq. [29]):

$$R_{ph} \approx R_B\frac{1+\alpha}{\ln(\lambda/R_B)} \quad (37)$$

whenever $R_B \ll \lambda$. The photospheric temperature $T_{ph} \equiv T(R_{ph})$ is offset from T_0 by

$$\frac{T_{ph} - T_0}{T_0} \approx \frac{R_L^2}{4R_{ph}^2} \approx \left[\frac{\ln(\lambda/R_B)}{2(1+\alpha)}\frac{R_L}{R_B}\right]^2 \ll 1, \quad (38)$$

while the photospheric pressure $P_{ph} \equiv P(R_{ph})$ is

$$P_{ph}/P_0 \approx (\lambda/R_B)^{1/(1+\alpha)} \gg 1. \quad (39)$$

Below the photosphere we again use equations (6) and (9). Similar to equation (27), one finds

$$\left(\frac{P}{P_0}\right)^{1+\alpha} - \left(\frac{P_{ph}}{P_0}\right)^{1+\alpha} = \frac{\nabla_0}{\nabla_\infty}\left[\left(\frac{T}{T_0}\right)^{4-\beta} - \left(\frac{T_{ph}}{T_0}\right)^{4-\beta}\right], \quad (40)$$

where boundary conditions $P = P_{ph}$ at $T = T_{ph}$ were used. While $|T - T_0|/T_0 \lesssim 1$, the density profile is still given by equation (29), and for $r \lesssim R_{ph}$ equation (40) yields

$$\frac{T - T_{ph}}{T_0} \approx \frac{\nabla_\infty}{(1+\alpha)}\left\{\exp\left[(1+\alpha)\frac{R_B}{r}\right] - \left(\frac{P_{ph}}{P_0}\right)^{1+\alpha}\right\}, \quad (41)$$

where we took into account that $R_B/R_{out} \lesssim 1$. Keeping in mind that according to equations (24) and (39) $(P_{ph}/P_0)^{1+\alpha} \ll R_B\lambda/R_L^2$, one again finds that T starts to deviate significantly from T_0 at $r = R_a$, analogous to the optically thick case. Thus, under assumption (24) thermal transition occurs deep inside the envelope, always below the photosphere (see eq. [37]).

[7] The outer optically thick region can only exist if $\lambda \lesssim h$ so that nebula is homogeneous on scales $\sim\lambda$, which is not the case far from the star. This, however, turns out not to be important.

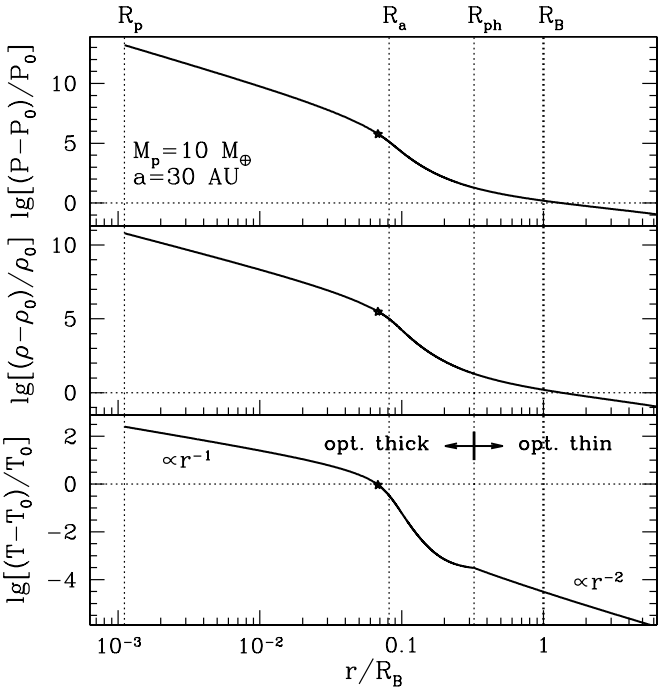

FIG. 4.—Same as Fig. 3, but for $M_p = 10\ M_\oplus$ at 30 AU. In this particular case $P_0 = 4 \times 10^{-10}$ bar, $\rho_0 = 2 \times 10^{-13}$ g cm^{-3}, and $T_0 = 55$ K. In addition, $\lambda > R_B$ and $R_B\lambda/R_L^2 \approx 2 \times 10^5$, i.e., the envelope has an outer optically thin region and possesses an outer radiative zone (see § 3.2). The rest of notation is the same as in Fig. 3.

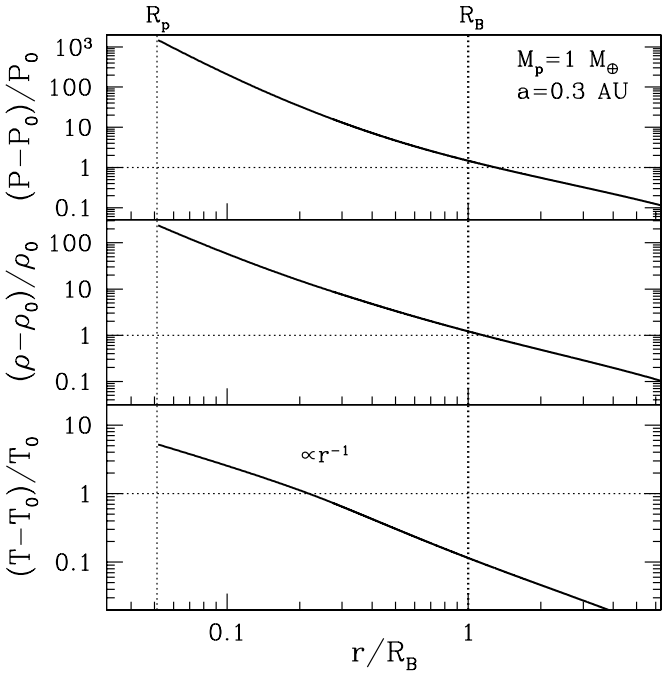

FIG. 5.—Same as Fig. 3, but for $M_p = 1\ M_\oplus$ at 0.3 AU. In this particular case $P_0 = 10^{-3}$ bar, $\rho_0 = 7 \times 10^{-8}$ g cm^{-3}, and $T_0 = 550$ K. In addition, $\lambda \ll R_B$ and $R_B\lambda/R_L^2 \approx 0.15$, i.e., the envelope is optically thick everywhere and possesses an outer convective zone (see § 4). The interior of this atmosphere is also convective for a particular choice of gas parameters (the same as for Fig. 3) used in producing this figure.

In the deep atmosphere ($r \lesssim R_a$) $T(r)$ and $P(r)$ are again given by equations (33) and (34). Thus, despite some differences in the structure of the upper atmosphere ($r \gtrsim R_a$) in the optically thin and thick cases, the structure of the inner atmosphere is the same. Figure 4 displays properties of an atmosphere around a 10 $M_\oplus$ core at 30 AU (for which eq. [24] is valid). In the optically thin region $T(r)$ was calculated using equation (35), and all input parameters (e.g., opacity, accretion regime, and γ) are the same as those used for Figure 3.

3.3. *Convection in the Deep Atmosphere*

We have previously demonstrated that the outer atmospheres of low-luminosity cores ($r \sim R_B$) are convectively stable, and our calculations in §§ 3.1 and 3.2 have assumed radiative energy transfer. In this section we determine under which circumstances deep atmosphere may become convective and also calculate the envelope structure in convectively unstable regions.

In the optically thick case investigated in § 3.1 one finds using equations (25) and (27) that

$$\nabla(T) = \nabla_0 \left[1 - \left(\frac{T_0}{T}\right)^{4-\beta} \left(1 - \frac{\nabla_\infty}{\nabla_0}\right)\right] \tag{42}$$

$$\approx \nabla_0 \left[1 - \left(\frac{T_0}{T}\right)^{4-\beta}\right], \tag{43}$$

where we took equation (23) into account. Thus, outside of R_a, where $T \approx T_0$, the temperature gradient is small and the atmosphere is convectively stable, justifying the results for the structure of the upper atmosphere obtained in § 3.1. Equation (43) clarifies the meaning of constant ∇_0, which is simply the temperature gradient in the deep atmosphere where $T \gg T_0$.

A similar situation is found in the optically thin case (see § 3.2). Above the photosphere $T \approx T_0$ (see eqs. [36] and [38]), while the pressure profile is given by equation (29). Then one obtains from equation (25) that

$$\nabla \approx \frac{1}{4}\left(2\frac{R_L^2}{R_B r} + 3\frac{R_L^2}{R_B \lambda}\right) \ll 1, \tag{44}$$

i.e., that the atmosphere is definitely convectively stable above the photosphere. Below the photosphere, for $r \lesssim R_{ph}$, the relation between T and P is given by equation (40), which leads to

$$\nabla(T) = \nabla_0 \left\{1 - \left(\frac{T_{ph}}{T}\right)^{4-\beta} \left[1 - \frac{\nabla_\infty}{\nabla_0}\left(\frac{P_{ph}}{P_0}\right)^{1+\alpha}\left(\frac{T_0}{T_{ph}}\right)^{4-\beta}\right]\right\}. \tag{45}$$

Since according to equations (38) and (39) $T_{ph} \approx T_0$ and $(P_{ph}/P_0)^{1+\alpha} \approx \lambda/R_B$, one finds that ∇ is still given by equation (43) below R_{ph} with the relative accuracy $O(R_L^2/R_B^2) \ll 1$. Consequently, in the optically thin case covered by equation (24) the atmosphere is convectively stable everywhere above R_a, analogous to the optically thick case. Thus, in both cases considered in §§ 3.1 and 3.2 the upper atmosphere is radiative.

Deep inside the atmosphere $\nabla \to \nabla_0$ (see eq. [43]). Thus, whenever

$$\nabla_0 < \nabla_{ad}, \tag{46}$$

the *whole* atmosphere is convectively stable (assuming that γ and ∇_{ad} are constant throughout the atmosphere; see § 6.3) and energy is transferred from its bottom by radiation. For the constant opacity ($\alpha = \beta = 0$) one finds that $\nabla_0 = 1/4$ (Stevenson

1982) and the envelope is convectively stable provided that it is composed of monatomic or diatomic gas.

In the opposite case, when $\nabla_0 > \nabla_{\rm ad}$, the envelope becomes convectively unstable when T reaches

$$T_{\rm conv} \approx T_0 \left(1 - \frac{\nabla_{\rm ad}}{\nabla_0}\right)^{-1/(4-\beta)}. \quad (47)$$

This critical temperature is not very different from T_0, meaning that $T_{\rm conv}$ is achieved at $r \approx R_a$. Thus, the atmosphere of a low-luminosity core can become convective only below $\approx R_a$. When the dominant source of opacity in the outer atmosphere is dust with $\beta = 1$, the atmosphere is convectively unstable if H_2 is its major constituent. In this case convection sets in at $T_{\rm conv} = 7^{1/3} T_0 \approx 1.9 T_0$. The edge of the convection zone as shown in Figures 3 and 4 agrees with this estimate.

The convective part of the atmosphere cannot be described by equation (9). Instead, one uses equation (11) to relate P and ρ in equation (6). The polytropic constant K in equation (11) is set by the conditions at the edge of the convection zone, i.e., at $T = T_{\rm conv}$. In the optically thin case equation (40) sets the pressure at this point as

$$P_{\rm conv} \equiv P_0 \left\{ \left(\frac{P_{\rm ph}}{P_0}\right)^{1+\alpha} + \frac{\nabla_0}{\nabla_\infty} \left[\frac{1}{1 - \nabla_{\rm ad}/\nabla_0} - \left(\frac{T_{\rm ph}}{T_0}\right)^{4-\beta} \right] \right\}^{1/(1+\alpha)} \approx P_0 \left[\frac{\nabla_{\rm ad} \nabla_0}{\nabla_\infty (\nabla_0 - \nabla_{\rm ad})} \right]^{1/(1+\alpha)}. \quad (48)$$

The last line in equation (48) follows from equation (39) and $T_{\rm ph} \approx T_0$. Apparently, $P_{\rm conv} \sim P_a \gg P_0$ (see eq. [32]). In the optically thick case $P_{\rm conv}$ is related to $T_{\rm conv}$ by equation (27). Using this fact one can easily see that $P_{\rm conv}$ is still given by the last line in equation (48), despite the different structure of the outer radiative layer.

Solving equations (6) and (11) with the boundary condition $\rho = \rho_{\rm conv} \equiv P_{\rm conv} \mu / k T_{\rm conv}$ at $r \approx R_a$ and using $K = P_{\rm conv} \rho_{\rm conv}^{-\gamma}$, one finds

$$\rho(r) = \rho_{\rm conv} \left[1 + \nabla_{\rm ad} \frac{G M_p}{K \rho_{\rm conv}^{\gamma-1}} \left(\frac{1}{r} - \frac{1}{R_a} \right) \right]^{1/(\gamma-1)} = \rho_{\rm conv} \left[1 + \nabla_{\rm ad} \left(1 - \frac{\nabla_{\rm ad}}{\nabla_0}\right)^{1/(4-\beta)} \left(\frac{R_{\rm B}}{r} - \frac{R_{\rm B}}{R_a} \right) \right]^{1/(\gamma-1)}. \quad (49)$$

For $r \lesssim R_a(1 - R_a/R_{\rm B})$ one finds $\rho \gg \rho_{\rm conv}$ and

$$\left(\frac{\rho}{\rho_{\rm conv}}\right)^{\gamma-1} \approx \frac{T}{T_{\rm conv}} \approx \nabla_{\rm ad} \frac{T_0}{T_{\rm conv}} \left(\frac{R_{\rm B}}{r} - \frac{R_{\rm B}}{R_a} \right). \quad (50)$$

Comparing $T(r)$ from equation (50) with equation (33), one concludes that the temperature profile in the deep atmosphere is not very sensitive to the details of the atmospheric structure.

4. ATMOSPHERES WITH OUTER CONVECTIVE ZONE

Whenever the planetesimal accretion luminosity is so high that $R_L \gtrsim (R_{\rm B}\lambda)^{1/2}$ in the optically thick case or $R_L \gtrsim R_{\rm B}$ in the optically thin case, the assumptions used in §§ 3.1 and 3.2 break. Based on the results of § 3, we anticipate that the intense energy release at the core surface strongly affects the gas temperature even outside the Bondi sphere, which qualitatively changes the atmospheric structure. Such cores will be referred to as "high-luminosity" cores. We concentrate on the optically thick case for which

$$R_{\rm B} \gg \lambda, \quad R_L^2 \gtrsim R_{\rm B}\lambda \quad (51)$$

(directly opposite to eq. [23]), typical for the terrestrial region (see Fig. 2).

It is clear from equations (25) and (26) that under these conditions $\nabla_\infty \gtrsim \nabla_{\rm ad}$, so that gas cannot be convectively stable even outside the Bondi sphere, at $r \gtrsim R_{\rm B}$: the large energy flux due to planetesimal accretion considerably affects T even beyond the Bondi radius, where P is almost constant and equal to its nebular value P_0. As a result, the stability condition in equation (8) is violated and the atmosphere acquires an *outer convective zone*. This is in contrast to the low-luminosity cores typical for the region of giant planets, which always have atmospheres possessing an almost isothermal outer radiative zone (see § 3).

A calculation similar to that leading to equation (49) yields the following density structure in the outer convective part of the atmosphere:

$$\rho(r) = \rho_0 \left[1 + \nabla_{\rm ad} \left(\frac{R_{\rm B}}{r} - \frac{R_{\rm B}}{R_{\rm out}} \right) \right]^{1/(\gamma-1)}. \quad (52)$$

This expression shows that ρ, P, and T deviate by a factor of ~ 1 from ρ_0, P_0, T_0 at $r \sim R_{\rm B}$, and then increase as some powers of $R_{\rm B}/r$ inside the Bondi sphere. The atmospheric structure is rather insensitive to a particular choice of $R_{\rm out}$ where the boundary conditions (22) are set, as long as $R_{\rm out} \gtrsim R_{\rm B}$.

The deep atmosphere can be either convective or radiative depending on the relationship between ∇_0 and $\nabla_{\rm ad}$, as described in § 3.3: the atmosphere is convective from $R_{\rm out}$ all the way to R_p when $\nabla_0 > \nabla_{\rm ad}$ (assuming that α, β, and γ are the same in the whole atmosphere), but convection stops and the atmosphere develops an inner radiative zone at some depth $r = R_{\rm rad}$ if $\nabla_0 < \nabla_{\rm ad}$. In the latter case the pressure $P_{\rm rad}$, temperature $T_{\rm rad}$, and density $\rho_{\rm rad}$ at the point of transition are given as functions of $R_{\rm rad}$ by equation (52), since the outer boundary of the radiative zone is also the inner boundary of the convective zone. Within the radiative zone $\nabla(T)$ is given by equation (45) with $P_{\rm ph}$ and $T_{\rm ph}$ replaced by $P_{\rm rad}$ and $T_{\rm rad}$. The condition $\nabla(T_{\rm rad}) = \nabla_{\rm ad}$ then fixes the value of $R_{\rm rad}$:

$$R_{\rm rad} \approx R_{\rm B} \frac{\nabla_{\rm ad}}{\Theta}, \quad \Theta \equiv \left(\frac{\nabla_\infty}{\nabla_{\rm ad}} \right)^{\nabla_{\rm ad}/[(4-\beta)(\nabla_{\rm ad} - \nabla_0)]}. \quad (53)$$

Clearly $R_{\rm rad} \ll R_{\rm B}$, because $\nabla_\infty \gg 1$ and $\Theta \gg 1$ for high-luminosity cores. The inner radiative zone exists only if $R_{\rm rad} > R_p$ in addition to $\nabla_0 < \nabla_{\rm ad}$. Of course, T and ρ at $R_{\rm rad}$ are much larger than T_0 and P_0: $T_{\rm rad}/T_0 = (\rho_{\rm rad}/\rho_0)^{\gamma-1} \approx \Theta$ (see eq. [52]).

Properties of an atmosphere around a 1 $M_\oplus$ core at 0.3 AU (for which the condition [5] is fulfilled) are displayed in Figure 5. Calculation assumes the same choice of gas parameters as used in producing Figure 3, which results in a fully convective atmosphere. Note the difference in atmospheric structure compared to Figures 3 and 4, caused by the assumption of a high-luminosity core.

For completeness we also mention the optically thin case

$$R_{\rm B} \ll \lambda, \quad R_{\rm B} \ll R_L, \tag{54}$$

opposite to that considered in § 3.2. This particular relationship between $R_{\rm B}$, R_L, and λ can be realized only in the region of giant planets for small cores accreting in the fast regime (see Fig. 2). Using equation (36) one finds T to be strongly perturbed even outside the Bondi sphere, because $R_{\rm B} \ll R_L$. It is rather clear that such atmospheres would possess outer convective zones, similar to the optically thick case in equation (51). This conclusion is independent of the relationship between R_L and λ.

5. MASS OF THE ATMOSPHERE AND CRITICAL CORE MASS

We define the mass of the atmosphere $M_{\rm atm}$ as

$$M_{\rm atm} \equiv 4\pi \int_{R_p}^{R_{\rm B}} \rho(r') r'^2 \, dr', \tag{55}$$

where we have chosen $R_{\rm B}$ as the outer boundary of the envelope. We compute $M_{\rm atm}$ separately for atmospheres with the outer radiative and convective zones, since $M_{\rm atm}$ is very different in the two cases. These results allow us to estimate the critical core mass $M_{\rm cr}$ necessary for the initiation of a runaway gas accretion in § 5.3.

5.1. *Mass of a Low-Luminosity Atmosphere*

The results of § 3 allow us to calculate the mass of an atmosphere around a low-luminosity core:

$$M_{\rm atm} \approx 4\pi \Psi_1 \rho_0 R_{\rm B}^3 \left(\frac{R_{\rm B}\lambda}{R_L^2} \right)^{1/(1+\alpha)} \tag{56}$$

(see Appendix B for details), where Ψ_1 is a weak (logarithmic) function of $R_{\rm B}\lambda/R_L^2$ given by equation (B1). This expression is valid provided that the atmospheric mass is mainly contributed by gas at $r \sim R_a$, which is true for all atmospheres having either convective interiors with $\gamma > 4/3$ or radiative interiors with $\nabla_0 > 1/4$. In such atmospheres the innermost layers at $r \ll R_a$ provide subdominant contribution to $M_{\rm atm}$ (see Appendix B). We restrict ourselves to studying only atmospheres possessing this property (see § 6.3 for the discussion of other possibilities). Gas outside R_a is unimportant for calculation of $M_{\rm atm}$ as long as $\nabla_\infty \ll 1$ because of the exponential density profile for $r \gtrsim R_a$.

Atmospheres having opacity independent of pressure (and, consequently, density, i.e., $\alpha = 0$) possess an interesting property: regardless of whether the atmospheric interior is radiative or convective, $M_{\rm atm}$ is virtually independent of the temperature and density in the surrounding nebula. Indeed, using equations (14), (12), (17), (31), and (A1) one finds that

$$\begin{aligned} M_{\rm atm} &= 64\pi^2 \Psi_1 \left(\frac{G M_p \mu}{k} \right)^4 \frac{\sigma}{\kappa_0 L} \\ &\approx \left[\ln (\nabla_\infty^{-1}) \right]^{-1/2} \left(\frac{M_p}{M_\oplus} \right)^{8/3} \kappa_{0.1}^{-1} \\ &\times \begin{cases} 2.7 \, M_\oplus \, a_{10}^3, & \text{slow}, \\ 1.4 \times 10^{-3} \, M_\oplus \, a_{10}^2, & \text{intermediate}, \\ 3.2 \times 10^{-5} \, M_\oplus \, a_{10}^{3/2}, & \text{fast}. \end{cases} \end{aligned} \tag{57}$$

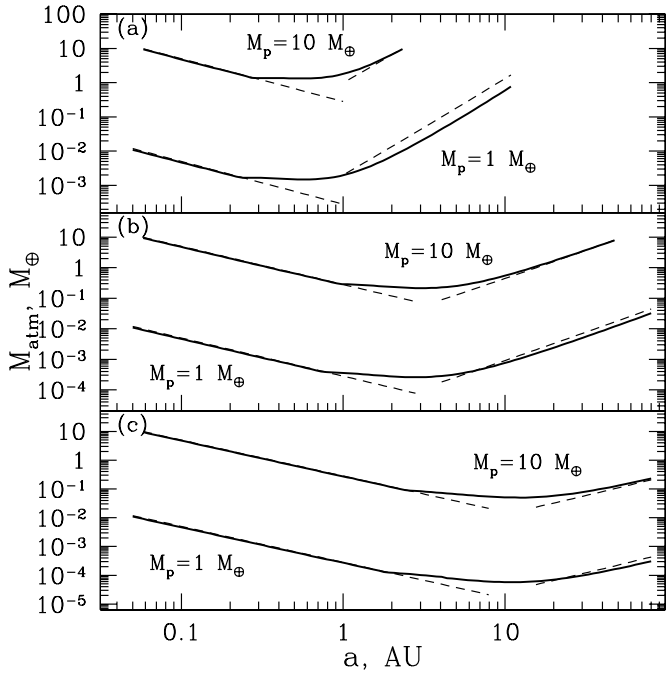

FIG. 6.—Mass of the atmosphere $M_{\rm atm}$ for two values of $M_p = 1$ and 10 $M_\oplus$ as a function of semimajor axis a. Different panels correspond to different planetesimal accretion regimes: (*a*) slow, (*b*) intermediate, and (*c*) fast. Solid curves labeled with corresponding core masses represent results of numerical calculation of $M_{\rm atm}$. Dashed lines display analytical estimates of $M_{\rm atm}$ for the same M_p given by eqs. (57) and (58) for large and small a, respectively.

Different numerical estimates are for the three accretion regimes described in Appendix A and assume molecular gas of the cosmic composition, $\beta = 1$, and $\gamma = 7/5$ (this choice of β and γ makes deep interior of the atmosphere convective; see § 3.3). Both T_0 and ρ_0 enter equation (57) only logarithmically through the dependence of Ψ_1 on $R_{\rm B}/R_a$ (see eqs. [31] and [B1]). Local conditions in the protoplanetary disk affect $M_{\rm atm}$ only through the gas opacity κ_0 and planetesimal accretion rate $\dot{M}$. This peculiarity was first noticed by Stevenson (1982), who discovered it while studying radiative atmospheres with constant gas opacity, $\alpha = \beta = 0$. Equation (57) demonstrates that insensitivity of $M_{\rm atm}$ to T_0 and ρ_0 is not limited to the case of radiative atmospheres with constant κ: it also holds for atmospheres with either convective or radiative interiors having temperature-dependent κ as long as $\alpha = 0$, i.e., κ is independent of ρ. When κ does depend on pressure ($\alpha \neq 0$), one finds $M_{\rm atm} \propto (\rho_0/T_0^3)^{\alpha/(1+\alpha)}$, i.e., the envelope mass does depend on the nebular properties in general.

It might seem surprising that the mass of an atmosphere with a convective interior is sensitive to radiative opacity κ_0, since below R_a energy is transported by convection. However, the properties of the convective interior are fully determined by the boundary conditions (gas entropy) set at the transition between the convective and radiative regions of an atmosphere. These conditions do depend on κ, since they are defined by the properties of the outer radiative region, which is generic for all low-luminosity cores (see § 3).

In Figure 6 we plot $M_{\rm atm}$ for cores of a given mass (1 and 10 $M_\oplus$) as a function of a for fast, intermediate, and slow planetesimal accretion regimes (see Appendix A). Numerical results of the envelope structure calculations for $\alpha = 0$, $\beta = 1$, $\kappa_0 = 0.1$ cm^2 g^{-1}, and $\gamma = 7/5$ are shown by solid curves; the dashed line at large a is our analytical estimate of $M_{\rm atm}$ given by equation (57). As Figure 6*a* demonstrates, formula (57) somewhat overestimates $M_{\rm atm}$ because of the finite size of the core: our extension of the

integration in equation (B1) to zero (instead of R_p) leads to an overestimate[8] of $M_{\rm atm}$.

5.2. *Mass of a High-Luminosity Atmosphere*

We calculate the mass of an atmosphere around a high-luminosity core using the density profile in equation (52):

$$M_{\rm atm} = 4\pi\Psi_2\rho_0 R_{\rm B}^3 \approx 2.8\times10^{-4}\ M_\oplus\left(\frac{M_p}{M_\oplus}\right)^3 a_1^{-5/4},$$
$$\Psi_2(\gamma) \equiv \int_0^1 z^2\left(1+\frac{\nabla_{\rm ad}}{z}\right)^{1/(\gamma-1)} dz, \qquad (58)$$

where we have assumed $R_{\rm B} \ll R_{\rm out}$ and the numerical estimate is for $\gamma = 7/5$ ($\Psi_2 \approx 0.88$). A similar expression for $M_{\rm atm}$ can be found in Wuchterl (1993). This calculation assumes that the atmosphere is convective all the way from $r = R_p$ to the Bondi radius (which requires $\nabla_0 > \nabla_{\rm ad}$). Most of the mass is in the outer part of the atmosphere (allowing setting the lower integration limit in the definition of Ψ_2 to zero) provided that $\gamma > 4/3$. However, formula (58) holds[9] even if $\nabla_0 < \nabla_{\rm ad}$ and the atmosphere has an inner radiative region, since this region has rather small extent (see eq. [31]). The analytical estimate in equation (58) is displayed in Figure 6 by the dashed line (terrestrial planet region, $\lesssim$1 AU).

Comparison of equations (56) and (58) shows that the atmosphere around a high-luminosity core is less massive than around a low-luminosity core of the same mass. The reason for this is that in the first case atmospheric gas has an entropy equal to that of the surrounding nebula, while in the second the atmosphere is separated from the nebula by nonisentropic radiative layer. Entropy experiences significant drop[10] in this layer, making the atmosphere around the low-luminosity core much denser than around the high-luminosity core.

A remarkable property of high-luminosity cores is that their atmospheres have masses comparable to the total mass of unperturbed nebular gas (with $\rho = \rho_0$) contained within their Bondi spheres. This is to be contrasted with atmospheres of the low-luminosity cores possessing outer radiative regions, which not only have $M_{\rm atm} \gg \rho_0 R_{\rm B}^3$ but also contain this mass within a volume smaller than $R_{\rm B}^3$ (see eq. [56]). Clearly, introduction of a high-luminosity core does not perturb the surrounding nebula nearly as much as implanting a low-luminosity core into the nebula.

5.3. *Critical Core Mass*

As mentioned in § 1, both numerical calculations and analytical arguments suggest that the phase of rapid gas accretion onto the protoplanetary core initiates when $M_{\rm atm} \sim M_p$. The exact ratio of the two masses at the onset of instability is uncertain and can be determined only after the envelope's self-gravity is self-consistently taken into account, which is beyond the scope of this study. Here we simply assume this critical ratio to be a free parameter $\eta \sim 1$, so that

$$M_{\rm atm}(M_{\rm cr}) = \eta M_{\rm cr}, \qquad (59)$$

where $M_{\rm cr}$ is the critical core mass at the onset of nucleated instability. For a fixed η condition (59) can be viewed as an equation for $M_{\rm cr}$.

In the low-luminosity case using equations (7), (57), and (A1) we find

$$M_{\rm cr} \approx \left[\frac{\eta\theta}{64\pi^2\Psi_1}\frac{\Omega\Sigma_p a\kappa_0}{\sigma G^3\ M_\odot^{1/3}}\left(\frac{k}{\mu}\right)^4\right]^{3/5}$$
$$\approx \eta_{0.3}^{3/5}\kappa_{0.1}^{3/5}\begin{cases} 0.26\ M_\oplus\ a_{10}^{-9/5}, & \text{slow,}\\ 25\ M_\oplus\ a_{10}^{-6/5}, & \text{intermediate,}\\ 240\ M_\oplus\ a_{10}^{-9/10}, & \text{fast,}\end{cases} \qquad (60)$$

where $\eta_{0.3} \equiv \eta/0.3$, θ is a parameter determining the efficiency of accretion (see Appendix A), and we have neglected logarithmic terms entering the expression for $M_{\rm atm}$ (see eq. [57]). The critical mass is smaller for larger a because of the rapid decrease of the planetesimal accretion rate $\dot{M}$ with a. Also note a strong dependence of $M_{\rm cr}$ on the mean molecular weight μ of the gas (Stevenson 1982). Convective erosion of the core and/or dissolution of infalling planetesimals in the atmosphere might increase μ and considerably lower $M_{\rm cr}$, promoting core instability.

The opacity κ that enters the expressions for $M_{\rm atm}$ and $M_{\rm cr}$ in equations (56) and (60) is the opacity in the outer radiative zone only; it is the radiation transfer in this region that determines the conditions in the deep atmosphere and, hence, the atmospheric mass. Since in the radiative zone $T \approx T_0$, we can be more confident that κ in this region (which is almost certainly due to dust, so that κ is independent of ρ) can be represented by a simple power-law dependence in equation (10), in contrast to the complicated behavior of the molecular opacity in the deep atmosphere. Thus, we expect our results for $M_{\rm atm}$ and $M_{\rm cr}$ in the low-luminosity case to be rather robust.

In the high-luminosity case

$$M_{\rm cr} = c_0^3\left(\frac{\eta}{4\pi\Psi_2\rho_0 G^3}\right)^{1/2} \approx 30\ M_\oplus\ \eta_{0.3}^{1/2} a_1^{5/8} \qquad (61)$$

(see eqs. [58] and [59]). Unlike equation (60), in this case $M_{\rm cr}$ decreases with decreasing a because ρ_0 rapidly increases toward the star. Introducing the Toomre stability parameter $Q \equiv \Omega c_0/(\pi G\Sigma_g)$, one can rewrite equation (61) as $M_{\rm cr} = (Q/4\Psi_2)^{1/2} M_{\rm tr}$ (see definition [19]). This implies that $M_{\rm cr} \gtrsim M_{\rm tr}$ in gravitationally stable protoplanetary disks[11] having $Q \gtrsim 1$, which violates our assumption (20). This inconsistency does not affect our estimate (58) of $M_{\rm atm}$ as long as $M_p \lesssim M_{\rm tr}$, but it becomes a problem for more massive cores. As a result, equation (61) can give only a very rough estimate of $M_{\rm cr}$ (one can be certain that $M_{\rm cr}$ is larger than the transitional mass $M_{\rm tr}$ in this regime), since the nebula cannot be considered static and homogeneous on the scale of $R_{\rm B}$ (as we have always assumed) when $M_p > M_{\rm tr}$ (see § 2.2).

We plot $M_{\rm cr}$ as a function of a in Figure 7 for different planetesimal accretion regimes, self-consistently taking into account the transition between different types of atmospheres in the inner and outer parts of the protoplanetary disk. In addition to the results of numerical calculations of the atmospheric structure, we plot analytical approximations for $M_{\rm cr}$ given by equation (61) in the region of terrestrial planets[12] and by equation (60) in the

[8] The relative correction to $M_{\rm atm}$ in this case, $\sim(R_p/R_a)^{1/2}$, is small but sometimes nonnegligible. This discrepancy goes away when we artificially set $R_p = 0$ in our numerical calculations.

[9] Provided that $1/4 \le \nabla_0 \le \nabla_{\rm ad}$, since in this case the mass of the inner radiative region is finite as $r \to 0$ (see Appendix B).

[10] For instance, in the optically thick atmosphere around a low-mass core with $R_L^2/R_{\rm B}\lambda \approx \nabla_\infty \ll 1$, the adiabatic constant K at R_a is $K \sim K_0\nabla_\infty^{(\gamma-1)/(1+\alpha)}$ (see eqs. [47], [48], and [49]), where $K_0 \equiv P_0\rho_0^{-\gamma}$ is the adiabatic constant of the gas in the surrounding nebula. Clearly, $K \ll K_0$, so that the entropy of the gas in the inner atmosphere is *much lower* than in the surrounding nebula.

[11] A similar argument was advanced in Ikoma et al. (2001).

[12] We are using eq. (61) just to get a general idea of the behavior of $M_{\rm cr}$, hoping that it is not very much different from the real value of $M_{\rm cr}$.

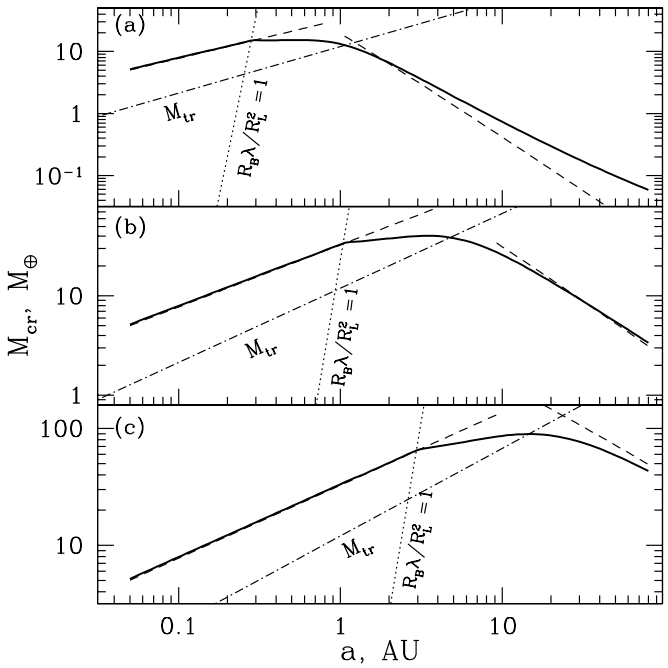

FIG. 7.—Critical core mass M_{cr} as a function of semimajor axis a for (*a*) slow, (*b*) intermediate, and (*c*) fast planetesimal accretion rates. Solid curves represent numerical results, while dashed lines display estimates of M_{cr} given by eqs. (60) and (61) at large and small a, respectively. The dot-dashed line shows the run of the transitional mass M_{tr} (eq. [19]) with a.

region of giant planets. In the terrestrial planet region one finds $M_{cr} > M_{tr}$, because the protoplanetary disk is very stable: $Q \gtrsim 30$ at $a \lesssim 1$ AU for the MMSN parameters given by equation (2). In the giant planet region there are discrepancies between the theory and numerical results at large a that are especially pronounced in Figure 7*a*. They appear because of the nonzero R_p causing equation (57) to overestimate M_{atm} (see § 5.1). More careful numerical calculation requires a bigger core for triggering runaway gas accretion.

6. DISCUSSION

The major result of our study is a clear distinction between protoplanetary atmospheres around high- and low-luminosity protoplanetary cores. Atmospheres of the first type have an outer convective region that smoothly merges with the surrounding nebula, effectively transmitting the nebular conditions to the atmospheric interior. Atmospheres of the second type possess an outer radiative zone isolating the dense and hot interior from the nebula. A specific type of atmosphere around a given core is determined solely by the relationships between the three important length scales, R_B, R_L, and λ, provided that the core mass satisfies the mass constraint in equation (20).

The segregation of atmospheres into two major classes depends to some extent on whether the upper atmosphere is optically thick or thin. In the optically thick case the atmospheric structure depends only on the dimensionless parameter $R_L^2/\lambda R_B$, roughly the radiative temperature gradient far from the core ∇_∞ (see eq. [26]), and is completely insensitive to the individual relationships between λ, R_L, and R_B as long as $\lambda \ll R_B$: the upper atmosphere is convective when $\nabla_\infty \gtrsim 1$ and radiative when $\nabla_\infty \lesssim 1$ (high- and low-luminosity cores, respectively). Wuchterl (1993) has formulated an analogous condition in terms of the nebular density ρ_0. In the optically thin case ($\lambda \gg R_B$) the separation between the two classes of atmospheres is somewhat more complicated (e.g., see constraint [24]) and depends on the individual relationships between λ, R_L, and R_B. The results of §§ 3 and 4 cover all possible cases and provide a useful classification scheme.

Because these characteristic length scales vary with the distance from the Sun, a specific type of atmosphere forming around a core of a given mass depends on a. Cores in the inner parts of protoplanetary disks ($a \lesssim 0.5$–2 AU depending on the planetesimal accretion regime) are typically of high luminosity ($R_L^2/R_B\lambda \gtrsim 1$), and their atmospheres possess an outer convective region (see Fig. 2, *top*). In the region of giant planets cores have low luminosity[13] ($R_L^2/R_B\lambda \lesssim 1$, since small $\dot{M}$ is lowering R_L while λ is very large), so that outside of ~0.5–2 AU protoplanetary atmospheres are massive with quite extended outer radiative zones (see Figs. 3 and 4).

6.1. *Comparison with Previous Studies*

Atmospheres with outer convective regions have been previously considered by Perri & Cameron (1974), Wuchterl (1993), and Ikoma et al. (2001), who found M_{atm} to be rather small, which translates into large M_{cr} (they find $M_{cr} \approx 60\ M_\oplus$). In addition, properties of such convective atmospheres were found to strongly depend on ρ_0 and T_0 in the surrounding nebula. This is exactly the picture that we described in § 4. Wuchterl (1993) suggested that the sensitivity to external conditions is a consequence of envelopes being *fully* convective, but we demonstrate in § 4 that the defining factor is convection in the *outermost* part of the atmosphere only, independent of whether the atmospheric interior is convective or radiative. The outer convective region sets the entropy of the inner atmosphere equal to the high entropy of the nebular gas (which lowers M_{atm}), making the overall structure (and mass) of the atmosphere sensitive to ρ_0 and T_0. Our analysis demonstrates that Perri & Cameron (1974) and Wuchterl (1993) should not have assumed fully convective atmospheres at 5 AU, in the region of giant planets; they should in fact have outer radiative zones.

Atmospheres possessing an outer radiative region have been studied numerically by Harris (1978), Mizuno et al. (1978), and Hayashi et al. (1979). Mizuno (1980) and Stevenson (1982) were the first to notice that the existence of this region makes M_{cr} virtually independent of either ρ_0 or T_0, provided that the opacity in the upper atmosphere is constant ($\alpha = \beta = 0$). We demonstrated in § 5.1 that this property holds also in a more general case of $\alpha = 0$ and arbitrary β (opacity independent of only the gas density; see eq. [57]). Dust dominating[14] opacity in the outer radiative zone provides κ with $\alpha = 0$, which naturally makes M_{atm} and M_{cr} independent of ρ_0 and T_0 (except for the local value of opacity κ_0, which scales with T_0). This conclusion is also completely independent of the structure of the deep atmosphere ($r \lesssim R_a$), be it radiative or convective.

We found the deep atmosphere ($r \lesssim R_a$) to be radiative provided that α and β in equation (10) are such that condition (46) is fulfilled; if $\nabla_0 > \nabla_{ad}$, the inner atmosphere must be convective. Stevenson (1982) found the *entire* atmosphere to be radiative in his model assuming a constant opacity (in agreement with eq. [46]). However, the opacity in the upper atmosphere should

[13] Some exceptions are possible (e.g., cores having $R_B \ll \lambda$ and $R_B \ll R_L$ in the region of giant planets have convective outer atmospheres; see § 4 and Fig. 2), but they typically occur for rather small cores unable to retain massive atmospheres.

[14] Unless the dust opacity is very small, $\lesssim 10^{-2}$ cm^2 g^{-1}, in which case the molecular opacity due to H_2 and H_2O becomes important; see the opacity plots in Hayashi et al. (1979) and Mizuno (1980) and Figs. 3 and 4.

be dominated by dust grains, which yield $\alpha = 0$ and nonzero $\beta \approx 1$–2. Equation (46) demonstrates that the interiors of envelopes with temperature-dependent dust opacities in the upper atmosphere should be convective if the atmosphere is composed of diatomic gas with $\gamma = 7/5$.

Apparently, dust cannot dominate the opacity in the whole atmosphere; at large depths H_2 and H_2O molecular opacities become more important, and their behavior cannot be described by a simple power-law dependence in equation (10). According to Hayashi et al. (1979) and Mizuno (1980), the deep atmosphere is typically convective when molecular opacity dominates. In addition to molecular, these authors also considered a constant dust opacity (similar to Stevenson 1982), which had the effect of making the outer atmosphere, where dust dominates κ, radiative. In their case the transition between radiative and convective zones occurs quite deep in the atmosphere, far below what we call R_a (if it were not for the molecular opacity, the atmosphere would be fully radiative in their case). The presence of such an extensive radiative zone with a constant opacity increases $M_{\rm atm}$ and decreases $M_{\rm cr}$, since $\rho \propto r^{-3}$ in the radiative region (for $\alpha = \beta = 0$), so that atmospheric mass is evenly distributed in $\ln r$ (see Appendix B). This augments $M_{\rm atm}$ compared to the gas mass in the outermost layer near R_a by a logarithmic factor $\gtrsim 1$. However, if one uses a realistic T-dependent dust opacity in the upper atmosphere, then typically $\nabla_0 > \nabla_{\rm ad}$, and there is no radiative region below R_a; convection starts at small depth, right below R_a, and most of the atmospheric mass is concentrated near R_a (see Appendix B). This decreases $M_{\rm atm}$ and increases $M_{\rm cr}$ compared to the case studied by Hayashi et al. (1979), Mizuno (1980), and Ikoma et al. (2000). Convection starting at small depth also makes the details of molecular opacity deep inside the atmosphere irrelevant, as energy is not carried by radiation below R_a.

Previous studies of atmospheres with outer radiative zones (Hayashi et al. 1979; Mizuno 1980; Stevenson 1982; Nakazawa et al. 1985; Ikoma et al. 2000) have typically found $M_{\rm cr} \sim 10\,M_\oplus$, depending on κ_0 and $\dot{M}$. These authors always assumed constant $\dot{M}$, i.e., $M_p \propto \tau$, while we consider several possible accretion regimes, self-consistently accounting for the dependence of $\dot{M}$ on M_p and a. For the same core formation timescale our assumed accretion law $M_p \propto \tau^3$ (see Appendix A) yields a higher $\dot{M}$ at the end of the core formation phase than constant $\dot{M}$ does. This acts to increase $M_{\rm cr}$ in our case. If $\kappa_0 = 0.1$ cm^2 g^{-1} and nucleated instability sets in when $M_{\rm atm} \approx 0.3 M_p$, we find (see Fig. 7) that in the fast regime of planetesimal accretion $M_{\rm cr} \gtrsim 50\,M_\oplus$ at 5–10 AU. In the intermediate accretion regime $M_{\rm cr} \approx 30\,M_\oplus$ at 5–10 AU; $M_{\rm cr}$ drops to $\approx 1\,M_\oplus$ in this region in the slow accretion regime. For the same $\dot{M}$ and κ_0 Ikoma et al. (2000) found lower values of $M_{\rm cr}$ (sometimes by ~ 2) than obtained in this work, because they used a constant opacity in the outer atmosphere (which increases $M_{\rm atm}$; see above), while we use a T-dependent dust opacity. Our neglect of atmospheric self-gravity is another reason for this difference.

Stevenson (1982) was the first to notice that $M_{\rm cr}$ is a sensitive function of the atmospheric composition in his study of purely radiative atmospheres. Our equation (60) confirms and generalizes this observation: we find $M_{\rm cr} \propto \mu^{-12/5}$ for *any* envelope with the outer radiative zone independent of whether its interior is radiative or convective. Dissolution of infalling planetesimals, erosion of the core by vigorous convection, or evaporation of some volatile icy content of the core can increase μ and decrease $M_{\rm cr}$ considerably ("superganymedean puffballs"; Stevenson 1984). On the other hand, atmospheric enrichment in high-Z elements might also increase the opacity in the outer atmosphere, which can at least partially counteract the decrease of $M_{\rm cr}$ due to large μ.

6.2. *Implications for Planet Formation*

Very close to the star, in the region where "hot Jupiters" are discovered ($a \lesssim 0.2$ AU), protoplanetary cores have a high luminosity and $\nabla_\infty \sim R_L^2/R_{\rm B}\lambda \gtrsim 1$ (see Fig. 2). In this case[15] $M_{\rm cr} \approx 5\,M_\oplus$ at 0.1 AU. At the same time the amount of refractory material in the inner parts of protoplanetary disks is rather small, most likely less than several $M_\oplus$. In addition, it takes a very long time ($\sim 10^8$ yr; see Chambers 2001) to collect this material into $\sim 1\,M_\oplus$ cores, so that nebular gas would be gone (disappears within $\sim 10^7$ yr) even if the disk mass allows assembly of 5 $M_\oplus$ cores.

Another problem with high-luminosity cores in the region of "hot Jupiters" is that in gravitationally stable disks they can become unstable only when M_p exceeds the transitional mass $M_{\rm tr}$ (see the discussion after eq. [61]). However, already at $M_p \sim (0.2$–$0.5) M_{\rm tr}$ gap formation around the orbit of the core becomes important (Rafikov 2002), inhibiting the supply of gas to the growing protoplanet and presenting another obstacle for the viability of core instability in the inner solar system. These considerations support the idea according to which the "hot Jupiters" or their massive progenitor cores must have migrated to their present-day locations from elsewhere.

Although the masses of existing terrestrial planets are clearly too low to drive the nucleated instability, they were high enough to retain quite substantial atmospheres while the nebular gas was still around. A massive primordial atmosphere can cause severe blanketing and melting of the core surface, an effect that has first been considered by Hayashi et al. (1979). Our calculations demonstrate that $M_{\rm atm} = 4 \times 10^{21}$, 10^{25}, 3×10^{25}, and 3×10^{22} g for Mercury, Venus, Earth, and Mars, respectively. This is to be compared with the current atmospheric masses of these planets: no atmosphere on Mercury and 5×10^{23}, 5.2×10^{21}, and 6.5×10^{18} g on Venus, Earth, and Mars. Clearly, the primeval atmospheres of the terrestrial planets have been heavily depleted.

As demonstrated in § 6.1, in the region of giant planets $M_{\rm cr}$ sensitively depends on the accretion regime: at 10 AU $M_{\rm cr} \lesssim M_\oplus$ in the slow regime and $\gtrsim 50\,M_\oplus$ in the fast. Accumulation of the cores of giant planets in the solar system at 10 AU must have proceeded in the intermediate or fast accretion regime (or some combination of the two), because smaller $\dot{M}$ would not allow unstable cores to form before the nebula dissipation this far from the Sun. This translates into $M_{\rm cr} \sim 20$–$60\,M_\oplus$, which is higher than the present-day masses of the cores of giants: the mass of Jupiter's core is estimated to be $\lesssim 10\,M_\oplus$, while Saturn's core has mass between 10 and 25 $M_\oplus$ (Saumon & Guillot 2004). However, the initial core masses of these two planets could have been higher; their total masses in high-Z elements may be as high as 30–40 $M_\oplus$, because some refractory materials are dissolved in their envelopes. Transporting these elements from the core into the atmosphere would require efficient erosion and mixing process, such as vigorous convection (Stevenson 1982), and it is not clear at present whether this is possible.

If cores of giants were not more massive initially and subsequently eroded, then they were not large enough to trigger nucleated instability, and yet giant planets are composed mainly of gas. One way to resolve this paradox is to hypothesize that the nebular opacity κ_0 was lower than 0.1 cm^2 g^{-1}, which brings $M_{\rm cr}$ down (see eq. [60]). Another possibility is suggested by the observation that core formation in the intermediate or fast regime can take a rather short time, of the order of several Myr (see eq. [A2]). In

[15] An accurate value of $M_{\rm cr}$ in the terrestrial region can only be obtained after the effects of the vertical disk structure, differential shear, complicated flow geometry within the Hill sphere, etc., are properly included, because in this part of the protoplanetary disk $M_p > M_{\rm tr}$ (see § 2.2 and Fig. 7).

this case, after the core has been mostly formed and the accretion luminosity dropped, there was still enough gas around to grow a giant planet. As a consequence of the reduced $\dot{M}$, the atmosphere would cool, contract, and accumulate more gas until $M_{\rm atm}$ reached $\sim M_p$ and runaway gas accretion commenced. A similar scenario of "stalled planetesimal accretion" has been studied numerically by Pollack et al. (1996) and Ikoma et al. (2000).

The relatively small atmospheres of Uranus and Neptune (containing only 1–4 $M_\oplus$ of H and He) suggest that these planets never underwent nucleated instability, and that it may be possible for all the gas that we see now in Uranus and Neptune to have come from steady state atmospheres around several subcritical cores that were less massive than the present-day cores of the ice giants. In this case, after the nebula went away these (presumably sub–isolation mass) cores merged, possibly on a rather long (10^8–10^9 yr) timescale. According to Genda & Abe (2003, 2004), their atmospheres would be largely preserved as a result of such catastrophic impacts, and this would allow Uranus and Neptune to appear in their current form long after the gaseous nebula has dispersed. Alternatively, Uranus and Neptune could have reached the core instability stage, but only after the nebula was very strongly depleted. In the latter case, fast accretion leads to accumulation of cores of isolation mass (essentially the present-day mass of the ice giants) and to subsequent nucleated instability before the nebula completely disperses. However, if at that moment the nebula was depleted by less than 10^2–10^3, Neptune and Uranus would have had much higher gaseous masses than they do now.

6.3. *Validity of Assumptions*

Because of the inherently analytical nature of this study aimed at singling out the most important aspects of atmospheric structure, we have neglected a number of relevant phenomena that may be important in some cases. Among them are the dissolution of infalling planetesimals (Pollack et al. 1996), opacity jumps due to dust grain melting (Mizuno 1980), and increase of the planetesimal capture cross section caused by the presence of the atmosphere (Inaba & Ikoma 2003). We have also employed a set of simplifying assumptions, such as hydrostatic and thermal equilibrium of the atmosphere. In Appendix C we demonstrate that these assumptions are valid. Our treatment of convection relies on the absence of an entropy gradient in the convective regions, and in Appendix D we check whether this assumption is appropriate.

Throughout our study we have neglected the gas accretion luminosity L_g compared to the planetesimal accretion luminosity L. Energy stored in the atmosphere depends on M_p, which changes because of the planetesimal accretion. As a result, the energy of the atmosphere varies in time, giving rise to an additional luminosity L_g caused by *gas accretion*:

$$L_g \equiv \frac{\partial |E_{\rm tot}|}{\partial \tau} = \frac{\partial |E_{\rm tot}|}{\partial M_p} \dot{M} \sim \frac{|E_{\rm tot}|}{\tau_{\rm acc}}. \tag{62}$$

Using the definition of the thermal timescale $\tau_{\rm th}$ in equation (C2), we find that $L_g/L \sim \tau_{\rm th}/\tau_{\rm acc}$. Thus, whenever the quasi-stationary approximation (i.e., $\tau_{\rm th} \ll \tau_{\rm acc}$) is valid, the gas accretion luminosity L_g is *small* compared to the planetesimal accretion luminosity L, and we can safely neglect L_g. Analogously, mass accretion rate of gas $\dot{M}_{\rm atm} \sim \dot{M} \times (M_{\rm atm}/M_p)$ (see eqs. [57] and [58]) is always smaller than the planetesimal mass accretion rate $\dot{M}$ if $M_{\rm atm} \lesssim M_p$, i.e., whenever the core is subcritical, which agrees with the assumptions adopted in this study.

Our use of a simple power-law opacity in equation (10) may seem an oversimplification compared to other treatments (e.g., Mizuno 1980; Ikoma et al. 2000) employing realistic opacity tables. However, as mentioned previously, in the outer part of the envelope κ is expected to be dominated by dust, leading to a convective atmosphere inward from R_a (for $\beta \approx 1$–2), which obviates the need to know the behavior of molecular opacity at high temperatures and pressures. Only opacity in the outer radiative zone (which is likely due to dust) is important for determining atmospheric structure.

Grain evaporation can lead to sudden opacity changes at specific locations in the atmosphere. Where this happens gas tends to settle onto a new radiative zero solution corresponding to a lower opacity, having a higher pressure for the same temperature (see eq. [27]). From equation (27) it is then clear that an abrupt decrease of κ_0 (and, correspondingly, λ) creates a radiative layer in which T is roughly constant while P increases with depth until the atmosphere settles onto a new radiative zero solution corresponding to the lowered opacity (or becomes convective if the remaining dust grains have a favorable opacity). Ice grain evaporation can occur at rather low temperatures in the outer parts of the atmosphere. In this case $M_{\rm atm}$ should be calculated with the postevaporation opacity, lowered compared to κ_0 in the surrounding protoplanetary nebula, resulting in a somewhat lower $M_{\rm cr}$ (see eq. [60]). Evaporation of the remaining refractory grains deeper down might not be so crucial, because at the relevant temperatures ($\sim 10^3$ K) the gas opacity may be more important.

A significant effect on $M_{\rm atm}$ and $M_{\rm cr}$ may come from the change of the equation of state caused by dissociation and ionization at large depths. If corresponding changes of κ or γ are such that $M_{\rm atm}$ is still dominated by the outer part of the atmosphere ($r \sim R_a$), then $M_{\rm atm}$ and $M_{\rm cr}$ would not be strongly affected. This requires $\gamma > 4/3$ or $\nabla_0 > 1/4$ to hold everywhere in the convective/radiative interior (see Appendix B). Tajima & Nakagawa (1997) demonstrate that in some cases these conditions can be violated, causing $M_{\rm atm}$ to be dominated by the inner region near the core. This should increase $M_{\rm atm}$ and decrease $M_{\rm cr}$ by a factor equal to some power of $(R_a/R_p) \gg 1$ (see Appendix B).

7. CONCLUSIONS

We investigated the steady state structure of an atmosphere around a protoplanetary core immersed in the gaseous disk. Our major results can be summarized as follows.

Atmospheres split into those having an outer convective or radiative zone. The former have an entropy of the interior equal to the entropy of the surrounding nebular gas; the latter have an interior entropy that is much lower than the nebular entropy, owing to the thermal decoupling provided by the outer radiative region. The type of atmosphere around a given core is determined by the relationships between the Bondi radius $R_{\rm B}$, photon mean free path λ, and luminosity radius R_L. High-luminosity cores (high L, large R_L) possess atmospheres with convective outer regions, while low-luminosity cores form atmospheres with the outer radiative zone. For typical protoplanetary disk conditions high-luminosity cores are common in the region of terrestrial planets. In the region of giant planets cores possess atmospheres with the outer radiative zone. The structure of the atmospheric interior is determined by the dependence of the opacity on the gas temperature and pressure.

In the terrestrial region the critical core mass for nucleated instability $M_{\rm cr}$ depends only on the local values of the nebular gas density and temperature. In the region of giant planets $M_{\rm cr}$ is insensitive to either ρ_0 or T_0 whenever the opacity in the outer

radiative zone is independent of the gas pressure, because the outer radiative zone decouples the inner parts of the envelope from the nebular gas (irrespective of whether the atmospheric interior is radiative or convective). At the same time, $M_{\rm cr}$ is a strong function of accretion luminosity, opacity, and mean molecular weight. In the region of giant planets a typical value of $M_{\rm cr}$ is several tens of $M_\oplus$ (30–50 $M_\oplus$ at 5 AU) if planetesimal accretion was fast enough for the core to form prior to the gas dissipation. Close to the Sun, at $a \sim 0.1$ AU, $M_{\rm cr} \approx 5\ M_\oplus$, independent of the planetesimal accretion rate. This makes in situ formation of "hot Jupiters" by nucleated instability onto the locally formed protoplanetary cores very unlikely.

The results of this study are also important for understanding the ancient atmospheres of terrestrial planets, which must have been significantly depleted.

I am grateful for hospitality from the Kavli Institute for Theoretical Physics, where part of this work was done. Useful discussions with Doug Lin, Peter Goldreich, and Bruce Draine and comments from an unknown referee are thankfully acknowledged. The author is a Frank and Peggy Taplin Member at the IAS; he is also supported by the W. M. Keck Foundation and NSF grants PHY-0070928 and PHY99-0794.

APPENDIX A

SUMMARY OF THE CORE ACCRETION RATES

Following Rafikov (2004b), we take the core accretion rate to be

$$\dot{M} = \Omega \Sigma_p R_p R_{\rm H} \theta, \tag{A1}$$

where θ is a parameter set by a particular mode of accretion. In this work we consider the following three important accretion regimes.

The first one is characterized by $\theta \approx p \ll 1$ (see definition [16]) and assumes that the core accretes planetesimals at a rate set by the core's geometric cross section $\sim R_p^2$. This regime is valid when the random epicyclic velocities of planetesimals are larger than the escape speed from the core's surface and gravitational focusing is weak. This "slow accretion" regime may take place after cores have reached the isolation mass by oligarchic growth (Chambers 2001; Goldreich et al. 2004).

The second regime of "intermediate accretion" takes place when random velocities of planetesimals are of the order of the shear velocity across the Hill radius of the core $\Omega R_{\rm H}$. In this case $\theta \approx 1$ and gravitational focusing is important. This regime corresponds to the boundary between the shear- and dispersion-dominated dynamical regimes (Stewart & Ida 2000) and may occur during oligarchic growth of protoplanetary embryos by accretion of large planetesimals (Kokubo & Ida 1998; Rafikov 2004b).

The third regime of "fast accretion" is characterized by $\theta \approx p^{-1/2}$ and is realized when the random velocities of planetesimals are so low that the planetesimal disk is geometrically very thin, essentially two-dimensional (see Rafikov 2004a, 2004b for the details of this scenario). This requires the planetesimal velocities to be smaller than $p^{1/2}\Omega R_{\rm H}$, meaning that some dissipative process such as gas drag effectively damps the planetesimal velocities. This can happen if fragmentation of large planetesimals in collisions at high velocities (induced by the gravity of protoplanetary cores) is capable of channeling a significant amount of mass initially locked up in large planetesimals into small debris for which the velocity damping time due to gas drag is shorter than the interval between consecutive approaches to cores (which do most of the dynamical stirring). Rapid decay of planetesimal random velocities caused by gas drag is a key factor in this regime. It allows small fragments to approach protoplanetary cores with very low velocities, allowing their efficient accretion and rapid growth of cores. Conventional treatment of planetesimal dynamics using azimuthal averaging of planetesimal velocities (Stewart & Wetherill 1988; Wetherill & Stewart 1989; Stewart & Ida 2000) conceals this complex behavior and does not allow fast accretion to take place even when fragmentation is properly accounted for. This is the reason for the difference between our results and those of Inaba et al. (2003), who included planetesimal fragmentation in their core accretion models but used azimuthally averaged stirring and damping rates when evolving the velocities of small planetesimals.

It is likely that each of these accretion regimes can take place during some stage of protoplanetary growth. A typical accretion timescale $\tau_{\rm acc}$ in each regime is

$$\tau_{\rm acc} \equiv \frac{M_p}{\dot{M}} = \frac{M_p}{\Omega \Sigma_p R_p R_{\rm H}} \theta^{-1} \approx \left(\frac{M_p}{M_\oplus}\right)^{1/3} \begin{cases} 3 \times 10^{10}\ {\rm yr}\ a_{10}^3, & \text{slow,} \\ 1.4 \times 10^7\ {\rm yr}\ a_{10}^2, & \text{intermediate,} \\ 3 \times 10^5\ {\rm yr}\ a_{10}^{3/2}, & \text{fast.} \end{cases} \tag{A2}$$

Note that in all three regimes listed above protoplanetary growth proceeds as $M_p \propto \tau^3$, where τ is the time.

APPENDIX B

MASS OF A LOW-LUMINOSITY ATMOSPHERE

As mentioned in § 5.1, most of the atmospheric mass is confined within R_a because ρ drops exponentially outside this radius, so that we may safely replace $R_{\rm B}$ with R_a in definition (55). Using equations (33) and (34) for radiative atmospheric interiors and equations (47), (48), and (50) for convective interiors, we arrive at result (56), in which Ψ_1 is defined as

$$\Psi_1(w, \zeta) \approx C \left(\frac{R_a}{R_{\rm B}}\right)^{3-\zeta} \int_0^1 z^2 \left(\frac{1}{z} - 1\right)^\zeta dz, \tag{B1}$$

where for atmospheres having a radiative interior ($\nabla_0 < \nabla_{\rm ad}$)

$$C = \left(\frac{4\nabla_0}{3}\right)^{1/(1+\alpha)} \nabla_0^{(1-\nabla_0)/\nabla_0}, \qquad \zeta = \frac{1}{\nabla_0} - 1, \tag{B2}$$

while in the case of an atmosphere having a convective interior ($\nabla_0 > \nabla_{\rm ad}$)

$$C = \left(1 - \frac{\nabla_{\rm ad}}{\nabla_0}\right)^{1/\nabla_{\rm ad}(4-\beta)} \left(\frac{4}{3}\frac{\nabla_0\nabla_{\rm ad}}{\nabla_0 - \nabla_{\rm ad}}\right)^{1/(1+\alpha)} \nabla_{\rm ad}^{1/(\gamma-1)}, \qquad \zeta = \frac{1}{\gamma - 1}. \tag{B3}$$

The constant ζ is a power-law index of the density dependence on $1/r$ (see eqs. [33], [34], and [49]).

Whenever $\zeta < 3$, the integral in equation (B1) is dominated by the contribution from $r \sim R_a$ and $M_{\rm atm}$ only weakly depends on the lower integration limit $R_p \ll R_a$ (this is why we set $R_p/R_{\rm B}$ to 0 in eq. [B1]). The condition $\zeta < 3$ is always satisfied for convective envelopes with $\gamma > 4/3$. In the radiative case one needs $\nabla_0 > 1/4$ for $\zeta < 3$. These are the types of atmospheres that we consider in this paper. Radiative envelopes with constant opacity ($\alpha = \beta = 0$) having $\nabla_0 = 1/4$ and $\zeta = 3$ contain equal amounts of mass for each decade in radius. In this case formula (56) still describes the behavior of $M_{\rm atm}$ but with $\Psi_1 \sim \ln(R_a/R_p)$ replacing equation (B1). This can considerably increase $M_{\rm atm}$, since $R_a \gg R_p$. If $\zeta > 3$, then $M_{\rm atm}$ is dominated by the innermost part of the atmosphere near R_p and depends on R_p: $M_{\rm atm} \propto (R_a/R_p)^{\zeta-3}$.

APPENDIX C

THERMAL TIMESCALE OF THE ENVELOPE

We calculate the thermal (Kelvin-Helmholtz) time for an atmosphere with the outer radiative zone (see § 3) and convective interior ($\alpha = 0$, $\beta = 1$, $\nabla_0 = 1/3 > \nabla_{\rm ad}$) with $\gamma = 7/5$. We define the thermal time as $\tau_{\rm th} \equiv |E_{\rm tot}|/L$, where $E_{\rm tot} = E_{\rm th} + E_{\rm gr}$ is the total energy contained within R_a, the sum of the thermal and gravitational energy of the envelope. It is easy to verify that $E_{\rm th} \sim |E_{\rm gr}|$, meaning that $E_{\rm tot} \sim E_{\rm gr}$ as well. We calculate $E_{\rm gr}$ using equations (47), (48), and (50):

$$\begin{aligned} E_{\rm gr} &= -\int_{R_p}^{R_a} G\frac{M_p}{r} 4\pi\rho(r) r^2\, dr \\ &\approx -4\pi P_0 R_{\rm B}^3 \left(\frac{R_{\rm B}}{R_p}\right)^{(3-2\gamma)/(\gamma-1)} \left[\frac{\nabla_{\rm ad}\nabla_0}{\nabla_\infty(\nabla_0 - \nabla_{\rm ad})}\right]^{1/(1+\alpha)} \frac{\gamma-1}{3-2\gamma} \left(1 - \frac{\nabla_{\rm ad}}{\nabla_0}\right)^{1/\left[\nabla_{\rm ad}(4-\beta)\right]} \nabla_{\rm ad}^{1/(\gamma-1)}. \end{aligned} \tag{C1}$$

This expression is valid for envelopes with convective interiors whenever $\gamma < 3/2$, in which case the gravitational energy budget is dominated by the *innermost* part of the envelope, near the core surface (see Harris 1978); this is why $E_{\rm gr}$ in equation (C1) explicitly depends on R_p. This would be different for atmospheres with convective interiors having $\gamma > 3/2$; then the energy content is dominated by the *outer* parts of the envelope[16] and is much smaller than that given by equation (C1). The energy is also small for envelopes having an outer convective zone; their energy is low because of the high interior entropy and associated low density. In a sense, the specific estimate (C1) of $E_{\rm gr}$ sets an upper limit on $\tau_{\rm th}$ and the degree of the envelope's deviations from the steady state.

Using our adopted values of γ, ∇_0, and $\nabla_{\rm ad}$ and the luminosity equations (7) and (A1), we find that

$$\tau_{\rm th} \approx \left(\frac{M_p}{M_\oplus}\right)^{5/3} \kappa_{0.1}^{-1} \begin{cases} 10^9 \text{ yr } a_{10}^{23/4}, & \text{slow}, \\ 10^3 \text{ yr } a_{10}^{15/4}, & \text{intermediate}, \\ 1 \text{ yr } a_{10}^{11/4}, & \text{fast}. \end{cases} \tag{C2}$$

Comparing this with equation (A2), one can see that typically $\tau_{\rm th} \ll \tau_{\rm acc}$, justifying our quasi-static approximation to the treatment of the atmospheric structure. Massive embryos ($M_p \gtrsim 10\ M_\oplus$) accreting in the slow regime at $a > 10$ AU should have this condition violated, and this may pertain to the development of nucleated instability in the region of giant planets (see § 6.2).

APPENDIX D

EFFICIENCY OF CONVECTIVE TRANSPORT

Our use of equation (11) assumes that convection is so efficient that even infinitesimal deviation of ∇ from $\nabla_{\rm ad}$ suffices to transport the energy flux produced at the core surface. If this is not the case, one should instead use the mixing-length theory (Kippenhahn &

[16] The latter is also true for envelopes with radiative interiors having $\nabla_0 > 1/3$ (which can exist only for $\gamma > 3/2$); most of the energy in the radiative envelopes with $\nabla_0 < 1/3$ is near the core.

Weigert 1990) to determine the value of ∇, and we check whether this is necessary. In light of the results of §§ 3.3 and 4, we describe the profiles of T, ρ, and P in the convective part of the atmosphere by

$$T = T_b\Phi, \qquad \rho = \rho_b\Phi^{1/(\gamma-1)}, \qquad P = P_b\Phi^{\gamma/(\gamma-1)}, \qquad \Phi \equiv 1 + \nabla_{\rm ad}\frac{T_0}{T_b}\left(\frac{R_{\rm B}}{r} - \frac{R_{\rm B}}{r_b}\right), \tag{D1}$$

where T_b, ρ_b, and P_b are values of T, ρ, and P at the boundary of the convective zone r_b. In the case of an atmosphere with the outer radiative zone studied in § 3.3, one finds $r_b = R_a$, $T_b = T_{\rm conv}$, $\rho_b = \rho_{\rm conv}$, and $P_b = P_{\rm conv}$, and equation (D1) reduces to equation (49). In the case of an atmosphere with the outer convective zone, $r_b = R_{\rm out}$, $T_b = T_0$, $\rho_b = \rho_0$, and $P_b = P_0$, and equation (D1) yields equation (52).

Following Kippenhahn & Weigert (1990), we introduce

$$x \equiv \nabla - \nabla_{\rm ad}, \qquad \nabla_{\rm rad} \equiv \frac{3}{16\pi\sigma G}\frac{\kappa LP}{M_pT^4}, \qquad U \equiv \frac{6\sqrt{2}\nabla_{\rm ad}}{\chi^2}\frac{\sigma T^4}{P\kappa\rho}\left(\frac{r^2}{GM_pH_p^3}\right)^{1/2},$$
$$W \equiv \nabla_{\rm rad} - \nabla_{\rm ad} = \nabla_{\rm ad}\left(\Phi^{(4-\beta)[(\nabla_0/\nabla_{\rm ad})-1]} - 1\right), \tag{D2}$$

where $\chi \sim 1$ is a mixing-length parameter, $H_p \equiv \partial r/\partial \ln P$ is the pressure scale height, and x is a deviation of the temperature gradient from $\nabla_{\rm ad}$, which has to be $\ll 1$ for equation (11) to apply. The value of x is determined by the following equation (Kippenhahn & Weigert 1990):

$$\left(\sqrt{x+U^2} - U\right)^3 = \frac{8}{9}U(W-x). \tag{D3}$$

A simple analysis demonstrates that $x \ll 1$ whenever either $W \ll 1$ or $W \ll U^{-1}$, and we look for conditions under which these restrictions are satisfied.

One expects deviations of x from zero to be most pronounced in the outer, low-density part of the atmosphere, where the radiative cooling time may become comparable to the eddy turnover time. Thus, we look at $r \approx R_a$ in the case of outer radiative zone, and $r \approx R_{\rm B}$ in the case of outer convective zone. In both cases $\Phi(r) \approx 1$. In the atmospheres of first type ($R_L^2 \ll R_{\rm B}\lambda$) we find (for $\alpha = 0$, $\beta = 1$, and $\gamma = 7/5$) using equations (47), (48), and (31) that

$$U(R_a) \approx \frac{6}{\chi^2}\frac{\sigma T_0^4}{c_0\kappa_0\rho_0^2GM_p}\left(\frac{R_L^2}{R_{\rm B}\lambda}\ln\frac{R_{\rm B}\lambda}{R_L^2}\right)^2$$
$$\approx \chi^{-2}\left(\frac{M_\oplus}{M_p}\right)^{1/3}\kappa_{0.1}\begin{cases} 3\times10^{-10}\ a_{10}^{-19/4}, & \text{slow,} \\ 3\times10^{-4}\ a_{10}^{-11/4}, & \text{intermediate,} \\ 0.2\ a_{10}^{-7/4}, & \text{fast.}\end{cases} \tag{D4}$$

In addition, $\nabla_{\rm rad} \sim \nabla_{\rm ad}$ at $r \lesssim R_a$, meaning that $W(R_a) \sim 1$ and $WU \sim U(R_a)$. Thus, in the region of giant planets ($a \gtrsim 5$ AU) $W \ll U^{-1}$, and convection is efficient for low-luminosity cores accreting planetesimals in the slow or intermediate regime. In the case of fast accretion, deviations of ∇ from $\nabla_{\rm ad}$ at the level of 0.1 might be expected in the outer atmosphere, at $r \approx R_a$.

In the case of high-luminosity cores ($R_L^2 \gg R_{\rm B}\lambda$), one finds an expression for $U(R_{\rm B})$ similar to equation (D4) but without $R_L^2/R_{\rm B}\lambda$ terms. In addition, $\nabla_{\rm rad} \sim R_L^2/R_{\rm B}\lambda \gg 1$ at $r = R_{\rm B}$. As a result,

$$U(R_{\rm B}) \approx \frac{0.2}{\chi^2}\left(\frac{M_p}{M_\oplus}\right)\kappa_{0.1}^{-1}a_1^{15/4},$$
$$W(R_{\rm B})U(R_{\rm B}) \approx 0.5\frac{L}{\rho_0c_0^3R_{\rm B}^2} \approx \chi^{-2}\left(\frac{M_\oplus}{M_p}\right)^{2/3}\begin{cases} 3\times10^{-4}\ a_1^{-1/2}, & \text{slow,} \\ 0.08\ a_1^{1/2}, & \text{intermediate,} \\ 1\ a_1, & \text{fast.}\end{cases} \tag{D5}$$

These estimates demonstrate that at $a \sim 0.1$ AU, where cores are likely of high luminosity, deviations from purely isentropic convection may only be important for the fast and intermediate accretion regimes.

REFERENCES

Chambers, J. E. 2001, Icarus, 152, 205
Genda, H., & Abe, Y. 2003, Icarus, 164, 149
———. 2004, Lunar Planet. Sci. Conf., 35, 1518
Goldreich, P., Lithwick, Y., & Sari, R. 2004, ApJ, 614, 497
D'Angelo, G., Henning, T., & Kley, W. 2002, A&A, 385, 647
D'Angelo, G., Kley, W., & Henning, T. 2003, ApJ, 586, 540
Draine, B. T. 2003, ARA&A, 41, 241
———. 2006, ApJ, 636, 1114
Harris, A. W. 1978, Lunar Planet. Sci. Conf., 9, 459
Hayashi, C., Nakazawa, K., & Mizuno, H. 1979, Earth Planet. Sci. Lett., 43, 22
Ikoma, M., Emori, H., & Nakazawa, K. 2001, ApJ, 553, 999
Ikoma, M., Nakazawa, K., & Emori, H. 2000, ApJ, 537, 1013
Inaba, S., & Ikoma, M. 2003, A&A, 410, 711
Inaba, S. S., Wetherill, G. W., & Ikoma, M. 2003, Icarus, 166, 46
Kippenhahn, R., & Weigert, A. 1990, Stellar Structure and Evolution (Berlin: Springer)

Kokubo, E., & Ida, S. 1998, Icarus, 131, 171
Lin, D. N. C., & Papaloizou, J. C. B. 1993, in Protostars and Planets III, ed. E. H. Levy & J. I. Lunine (Tucson: Univ. Arizona Press), 749
Mizuno, H. 1980, Prog. Theor. Phys., 64, 544
Mizuno, H., Nakazawa, K., & Hayashi, C. 1978, Prog. Theor. Phys., 60, 699
Nakazawa, K., Mizuno, H., Sekiya, M., & Hayashi, C. 1985, J. Geomagn. Geoelectr., 37, 781
Perri, F., & Cameron, A. G. W. 1974, Icarus, 22, 416
Pollack, J. B., Hubickyj, O., Bodenheimer, P., Lissauer, J. J., Podolak, M., & Greenzweig, Y. 1996, Icarus, 124, 62
Rafikov, R. R. 2002, ApJ, 572, 566
———. 2004a, in ASP Conference Ser. 316, Order and Chaos in Stellar and Planetary Systems, ed. G. G. Byrd et al. (San Francisco: ASP), 132
Rafikov, R. R. 2004b, AJ, 128, 1348
Sasaki, S. 1989, A&A, 215, 177
Saumon, D., & Guillot, T. 2004, ApJ, 609, 1170
Stevenson, D. J. 1982, Planet. Space Sci., 30, 755
———. 1984, Lunar Planet. Sci. Conf., 15, 822
Stewart, G. R., & Ida, S. 2000, Icarus, 143, 28
Stewart, G. R., & Wetherill, G. W. 1988, Icarus, 74, 542
Tajima, N., & Nakagawa, Y. 1997, Icarus, 126, 282
Tassoul, J.-L. 1978, Theory of Rotating Stars (Princeton: Princeton Univ. Press)
Wetherill, G. W., & Stewart, G. R. 1989, Icarus, 77, 330
Wuchterl, G. 1993, Icarus, 106, 323